12-18-2015

Chromatic Dispersion Compensation in electrical domain via Signal Pre-distortion using a dual-drive Mach-Zehnder Modulator

Saivivek Bheemanathini
sxb5542@rit.edu

Chromatic Dispersion Compensation in electrical domain via Signal Pre-distortion using a dual-drive Mach-Zehnder Modulator

Saivivek Bheemanathini

Dec 18,2015

Faculty Advisor: Prof. D.N.Maywar

Thesis committee

Mark Indelicato, Associate Professor

Sungyoung Kim, Ph.D. Assistant Professor

A thesis presented for the degree of

Master of Science

MS Telecommunications Engineering Technology Program

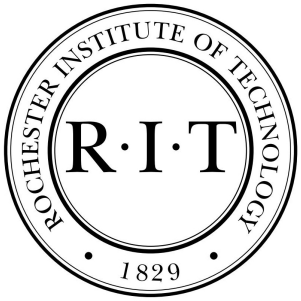

Electrical, Computer and Telecommunications Engineering Technology

College of Applied Science and Technology

Rochester Institute of Technology

Abstract

In recent years, evolution of technology has contributed a major role in the field of optical communication systems. There is an ever growing demand for transmitting signals at higher data rates and compensating the transmission impairments simultaneously. Speed of the signal transmission down the optical fiber is limited by transmission impairments that are characterized as linear or nonlinear losses. In my thesis, I lay a special emphasis on linear loss especially chromatic dispersion and it's effect on an optical signal down the fiber and study the compensation techniques in an electrical domain challenging the methods employed in an optical domain. In this digital world, there is an increase in the evolution of electrical components such as high speed memory units and low power consumption models. Electrical domain provides advantages in terms of processing the signal in a cost effective way and achieving the similar results with respect to the optical domain. In addition to the analysis, my investigation includes the effect of noise present in optical fiber communication systems and limitations of electrical components in achieving the compensation.

Contents

Chapter 1

Introduction

In this 20th century, technology in communications between two systems has been evolving at a faster rate to deliver data in a fast, efficient and secure manner. There is a lot of emphasis laid on two forms of signal propagation based on medium, such as wired and wireless transmissions. Both forms has its advantages and disadvantages, however, they are chosen in terms of speed, portability and security. In this paper, we study about the signal propagation in an optical fiber and an effective approach to mitigate linear chromatic dispersion by pre-distorting the signal at the transmitter in the electrical domain using a dual-drive Mach-Zehnder Modulator [1] .

In wired communications, optical fiber plays an important role is transmitting the data for long distances in the form of light. There are different types of fiber and fiber length can vary from few kilometers to thousands of kilometers. During it's propagation, transmission impairments will try to degrade the quality and limit the transmission distance in both linear and non-linear domain. Linear transmission impairments include dispersion, fiber loss, X-talk, accumulated amplified spontaneous emission (ASE) noise and polarization mode dispersion (PMD)[3]. In this thesis, we study to mitigate the transmission-related degradations that do not rapidly change in time in linear domain that includes chromatic dispersion a.k.a Group-velocity dispersion (GVD) leaving non-linear domain for future work.

In a fiber-optic telecommunications system, attenuation reduces the power of a

transmitted signal caused by media components such as cables, splicers and connectors and is significantly lower as compared to other media. And dispersion affects the transmission in two types: Chromatic Dispersion and Modal dispersion, where chromatic dispersion broadens the signal in the time-domain resulting in different speed of wavelengths and modal dispersion broadens the signal in time due to different propagation modes in an optical fiber. Modal dispersion plays a degrading role in multi-mode fiber whereas chromatic dispersion plays in single mode fiber that spreads the signal across long distances.

In contrast, Chromatic dispersion is deterministic, linear, and can be compensated. In digital communications, a bit sequence is represented as pulses and will spread large in time and merge due to chromatic dispersion making it difficult for the receiver to render the bit stream as shown in the Figure (1.1). This action limits the length of fiber that a signal can be sent down without amplification or regeneration.

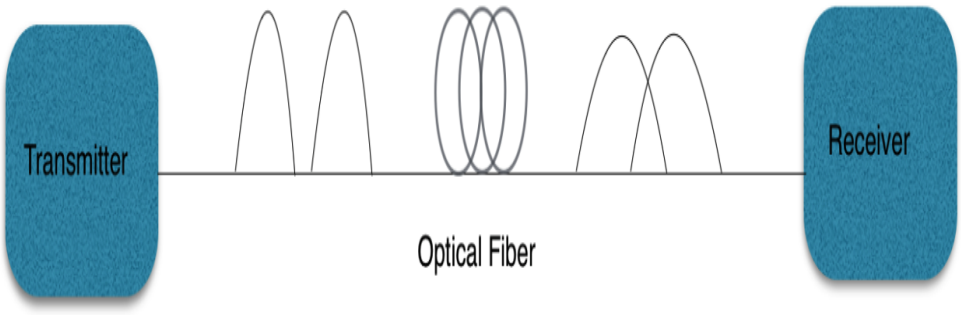

Figure 1.1: Pulse travels down the fiber and broadens in time domain

Further studies in the field of optical fiber communications contribute to the development of systems compensating the impairments in electrical domain in addition to optical domain. Electrical domain make use of digital signal processors such as ASIC, Xilinx,etc., CMOS units, D/A and A/D converters, etc. to achieve the compensation which is cost-cutting, ability to reproduce the signals efficiently and lot faster , more practical in terms of functionality as compared to use of costly optical fibers in optical domain dispersion compensation. Also, due to continuous

evolution in electrical instruments in terms of speed and reduction in power, electrical domain looks like a promising aspect to cut down the limitations set by the optical domain. [4]

In this thesis, we study the efforts to reduce the linear impairments and re-produce the novel technique discussed in IEEE paper "Electronic Dispersion Compensation by signal distortion using Digital processing and a Dual-drive MZM" and extend it's horizon by understanding the dependent nature of various optical parameters in different conditions. [1] To extend it's horizon, we have included noise in optical fiber communication systems such as thermal noise, shot noise and relative intensity noise (RIN) as a measure of performance of this pre-distortion technique with respect to the electrical parameters and its limitations.

Chapter 2

Forward Propagation

2.1 Basic Propagation

When an optical pulse propagates down the fiber, complex value of its electrical field $E(z, T)$ in time can be written in the form,

$$E(z, T) = \sqrt{P(t)} exp(i\phi), \tag{2.1}$$

and Phase is given by

$$\phi = \phi_0(t) + \omega t - \beta z. \tag{2.2}$$

where P is the power of the signal received by the photodiode at a distance z down the fiber, ϕ_0 is the initial phase, w is the angular frequency, and β is phase constant. In theory, optical signal property is activated by three factors, multiple transverse modes, multiple wavelengths and multiple polarization states and each individually or in combination are responsible for losses in the transmission impairments . However, in this paper, we consider a single mode fiber, and focus on single wavelength which play an important role to study the effect of chromatic dispersion, leaving effects of polarization dispersion for future work. [5]

In a single mode fiber, each spectral component has slightly different propagation constant, hence different phase velocities which is the main reason for the chromatic dispersion, which further illustrates the frequency dependent nature of an optical signal in the frequency domain. In spectral domain, with the introduction of Fourier transform, electrical field of an optical pulse is given by

$$E(z,T) = \frac{1}{2\pi}\int_{-\infty}^{\infty} E(z,\omega)\exp(-i\omega T)\,d\omega, \tag{2.3}$$

where $E(z,\omega)$ is the Fourier transform of the signal, in turn written as

$$E(z,\omega) = E(0,\omega)\exp(i\beta z). \tag{2.4}$$

and $E(0,\omega)$ is the Fourier transform of the signal $E(0,T)$ at $z = 0$.

2.2 Propagation constant β

Now, In general, propagation constant β in linear terms can be written in the form,

$$\beta_L(w) = \tilde{\eta}\omega\frac{\omega}{c}. \tag{2.5}$$

where c is velocity of light in vacuum and $\tilde{\eta}$ is a effective mode index as a function of carrier frequency ω that results in phase evolution for different spectral components leading to chromatic dispersion. Considering the frequency dependent nature of effective mode index, propagation constant β is expressed in the form of taylor series,

$$\beta_L(\omega) = \frac{1}{m!}\sum_{m=0}^{\infty}\frac{d^m\beta}{d\omega^m}(\omega-\omega_0)^m, \tag{2.6}$$

where ω_0 is the reference value of carrier frequency, and $\omega - \omega_0$ can be substituted as $\Delta\omega$ in the equation. Now further expanding the equation Eq(2.6), we get

$$\begin{aligned}\beta_L(\omega) &= \beta(\omega_0) + \frac{d\beta}{d\omega}\Delta\omega + \frac{1}{2}\frac{d^2\beta}{d\omega^2}(\Delta\omega)^2 + \frac{1}{6}\frac{d^3\beta}{d\omega^3}(\Delta\omega)^3 + ...,\\ &= \beta(\omega_0) + \beta_1\Delta\omega + \frac{1}{2}\beta_2(\Delta\omega)^2 + \frac{1}{6}\beta_3(\Delta\omega)^2 + ...,\end{aligned} \tag{2.7}$$

ignoring higher order terms, equation can be written as

$$\beta_L(\omega) = \beta\omega_0 + \beta_1\Delta\omega + \frac{1}{2}\beta_2(\Delta\omega)^2 + \frac{1}{6}\beta_3(\Delta\omega)^3. \tag{2.8}$$

where $\beta_1 = \frac{d\beta}{d\omega}$, $\beta_2 = \frac{d^2\beta}{d\omega^2}$, and $\beta_3 = \frac{d^3\beta}{d\omega^3}$ are orders of propagation constant β that are used to derive signal transmission. In this equation, β_1 is called first order of dispersion and is related as inverse of group velocity $\frac{1}{v_g}$ that accounts to a constant delay as signal propagates through an optical fiber and $\beta\omega_0$ does not contribute to dispersion due to absence of differential carrier frequency, however, second and third order of dispersion parameters β_2, β_3 are functions of carrier frequency and are responsible for broadening of signal pulse in an optical fiber. [4]

2.3 Non-linear Schrodinger Equation

In this paper, we lay a special emphasis on β_2 which is also called group as velocity dispersion parameter (GVD) and is expressed in the units of $[\frac{ps^2}{km}]$ and related chromatic dispersion parameter D, where $D = \frac{-2\pi c}{\lambda_0^2}\beta_2$ whose units are $[\frac{ps}{nm-km}]$. For a single mode fiber, at a wavelength of 1550 nm to the right of zero dispersion wavelength λ_{ZD}, Dispersion parameter D is found out to be 17 $[\frac{ps}{nm-km}]$.

[Note: Zero dispersion wavelength is defined as a wavelength at which dispersion parameter D is zero]. [1]

In fiber optics, wave propagation is modeled by the non-linear Schrodinger Equation (NSE). NSE describes the phenomena of transmission behavior of optical signal pulses through a nonlinear medium. Considering the propagation of optical signal in single-mode fibers and for pulse widths $> 5ps$, NSE is given by

$$i\frac{\partial A}{\partial z} = -\frac{i\alpha}{2}A + \frac{\beta_2}{2}\frac{\partial^2 A}{\partial T^2} - \gamma\left|A^2\right|A, \tag{2.9}$$

where A is the varying amplitude of the optical signal pulse and T is the time coordinate expressed in terms of group velocity v_g with respect to frame of reference t given by ($T = t - \frac{z}{v_g}$). This equation entails transmission impairments such as fiber losses, dispersion and nonlinear effects on pulses propagating along the fiber. Specifically, α is the attenuation constant responsible for fiber losses, β_2 is the GVD parameter responsible for pulse broadening and γ is the nonlinear parameter responsible for fiber nonlinearity.

2.3.1 Forward Propagation Equation and Transfer function

To obtain the effect of group-velocity dispersion in optical pulses transmitted along the fiber, a linear dispersive medium is considered. Nonlinear and fiber losses are ignored by setting the parameters $\gamma = 0$ and $\alpha = 0$ in Eq. (2.9).

The NSE becomes:

$$i\frac{\partial A}{\partial z} = \frac{\beta_2}{2}\frac{\partial^2 A}{\partial T^2}. \tag{2.10}$$

Eq.(2.10) can be solved using the Fourier Transform method. $A(z,\omega)$ is the Fourier transform of A(z,T) such that

$$A(z,T) = \frac{1}{2\pi}\int_{-\infty}^{\infty} A(z,\omega)\exp(-i\omega T)\,d\omega, \tag{2.11}$$

and

$$A(z,\omega) = \int_{-\infty}^{\infty} A(z,T)\exp(i\omega T)\,dT. \tag{2.12}$$

Applying the Fourier transform to the simplified NSE yields:

$$i\frac{\partial A}{\partial z} = -\frac{1}{2}\beta_2\omega^2 A. \tag{2.13}$$

Rearranging Eq. (2.13) yields:

$$\frac{\partial A}{A} = \frac{i}{2}\beta_2\omega^2\partial z. \tag{2.14}$$

Integrating Eq. (2.14) yields:

$$A(z,\omega) = A(0,\omega)\exp(\frac{i}{2}\beta_2\omega^2 z), \tag{2.15}$$

where $A(0,\omega)$ is the Fourier transform of the incident field at z=0. This Eq. (2.15) is our forward propagation equation. It propagates the light from z=0 to z. In other words, our transfer function is $H(\omega)$ given by

$$H = \exp(\frac{i}{2}\beta_2\omega^2 z) \tag{2.16}$$

and we can write

$$A(z,\omega) = A(0,\omega)H(\omega). \tag{2.17}$$

Eq. (2.17) is the final equation for the varying amplitude of signal pulse and shows that GVD changes the phase of the each spectral component of the pulse but the spectral pulse shape remain unaffected. Input pulses of arbitrary shapes can be assessed using the Eq. (2.15) and Eq (2.17).[1]

Combing Eq. (2.4) and Eq. (2.17), Electric field of an optical pulse at length z of an optical fiber in frequency domain is given by

$$E(z,\omega) = E(0,\omega)\exp(\frac{i}{2}\beta_2\omega^2 z). \tag{2.18}$$

2.4 Analysis

2.4.1 Analytical analysis

Let us consider the case of a Gaussian pulse for which incident field is of the form

$$A(0,T) = A_0 \exp(-\frac{T^2}{2T_0^2}), \tag{2.19}$$

where A_0 is the initial amplitude, T_0 is half-width at 1/e-intensity point, and it's relation with the full width half maximum (FWHM) for a Gaussian pulse is given by

$$T_{FWHM} = 2\sqrt{\ln 2}T_0. \tag{2.20}$$

The spectral amplitude of the incident field at z=0, $A(0,\omega)$ is given by

$$A(0,\omega) = \int_{-\infty}^{\infty} A(0,T)\exp(i\omega T)\,dT. \tag{2.21}$$

Using Eq. (2.15) and (2.19), the spectral amplitude of the incident field at z=z is given by

$$\begin{aligned} A(z,\omega) &= A(0,\omega)\exp(\frac{i}{2}\beta_2\omega^2 z), \\ &= \int_{-\infty}^{\infty} A(0,T)\exp(i\omega T)\,dT\exp(\frac{i}{2}\beta_2\omega^2 z), \\ &= \int_{-\infty}^{\infty} A_0\exp(-\frac{T^2}{2T_0^2})\exp(i\omega T)\,dT\exp(\frac{i}{2}\beta_2\omega^2 z), \\ &= \int_{-\infty}^{\infty} A_0\exp(-\frac{T^2}{2T_0^2}+i\omega T)\,dT\exp(\frac{i}{2}\beta_2\omega^2 z). \end{aligned} \tag{2.22}$$

Using the formulae in Fourier-Transforms,

$$\int_{-\infty}^{\infty} \exp(-ax^2 + bx)dx = \sqrt{\frac{\pi}{a}} \exp(\frac{b^2}{4a}). \tag{2.23}$$

Eq. (2.22) yields:

$$\begin{aligned} A(z,\omega) &= \int_{-\infty}^{\infty} A_0 \exp(-\frac{T^2}{2T_0^2} + i\omega T)\, dT \exp(\frac{i}{2}\beta_2\omega^2 z), \\ &= A_0 T_0 \sqrt{2\pi} \exp(-\frac{\omega^2 T_0^2}{2}) \exp(\frac{i}{2}\beta_2\omega^2 z), \end{aligned} \tag{2.24}$$

where $a = \frac{1}{2T_0^2}$ and $b = i\omega$.

$$A(z,\omega) = A_0 T_0 \sqrt{2\pi} \exp(-\frac{\omega^2 T_0^2}{2} + \frac{i}{2}\beta_2\omega^2 z). \tag{2.25}$$

Using Eq. (2.3), (2.23) and (2.25), the temporal amplitude of the Gaussian pulse obtained from the forward propagation equation is:

$$\begin{aligned} A(z,T) &= \frac{1}{2\pi} \int_{-\infty}^{\infty} A(z,\omega) \exp(-i\omega T)\, d\omega, \\ &= \frac{1}{2\pi} \int_{-\infty}^{\infty} A_0 T_0 \sqrt{2\pi} \exp(-\frac{\omega^2 T_0^2}{2} + \frac{i}{2}\beta_2\omega^2 z) \exp(-i\omega T)\, d\omega, \\ &= \frac{A_0 T_0}{\sqrt{2\pi}} \int_{-\infty}^{\infty} \exp[\frac{i\beta_2 z - T_0^2}{2}\omega^2 - i\omega T]\, d\omega. \end{aligned} \tag{2.26}$$

Using the formulae, take $a = (\frac{-i\beta_2 z + T_0^2}{2})$ and $b = -iT$, Eq.(2.26) yields:

$$\begin{aligned} A(z,T) &= \frac{A_0 T_0}{\sqrt{T_0^2 - i\beta_2 z}} \exp[-\frac{2T^2}{4(T_0^2 - i\beta_2 z)}], \\ &= \frac{A_0 T_0}{\sqrt{T_0^2 - i\beta_2 z}} \exp[-\frac{T^2}{2(T_0^2 - i\beta_2 z)}]. \end{aligned} \tag{2.27}$$

Note: if p= x+iy is a complex number, it's conjugate is given by $\tilde{p}$=x-iy; p.$\tilde{p}$ =

$x^2 + y^2$ and magnitude yields $|p| = \sqrt{x^2 + y^2}$.

Using the complex numbers formulae, we need to make the denominator free of complex terms. Now Eq. (2.27) can be written as

$$\begin{aligned} A(z,T) &= \frac{A_0 T_0}{\sqrt{T_0^2 - i\beta_2 z}} \exp[-\frac{T^2}{2(T_0^2 - i\beta_2 z)}], \\ &= \frac{A_0 T_0}{\sqrt{T_0^2 - i\beta_2 z}} \frac{\sqrt{T_0^2 + i\beta_2 z}}{\sqrt{T_0^2 + i\beta_2 z}} \exp[-\frac{T^2}{2(T_0^2 - i\beta_2 z)} \frac{T_0^2 + i\beta_2 z}{T_0^2 + i\beta_2 z}], \end{aligned} \tag{2.28}$$

where $x = T_0^2$ and $y = \beta_2 z$.

$$A(z,T) = \frac{A_0 T_0 \sqrt{T_0^2 + i\beta_2 z}}{\sqrt{T_0^4 + \beta_2^2 z^2}} \exp[-\frac{T^2(T_0^2 + i\beta_2 z)}{2(T_0^4 + \beta_2^2 z^2)}]. \tag{2.29}$$

We now seek to write A(z,w) as $A(z,w) = |A(z,w)| \exp(i\phi_A)$.

$$\begin{aligned} A(z,T) &= \frac{A_0 T_0}{\sqrt{T_0^4 + \beta_2^2 z^2}} \sqrt{\sqrt{T_0^4 + \beta_2^2 z^2} \exp\Big(i \arctan(\frac{\beta_2 z}{T_0^2})\Big)} \exp\Big(-\frac{T^2(T_0^2 + i\beta_2 z)}{2(T_0^4 + \beta_2^2 z^2)}\Big), \\ &= \frac{A_0 T_0}{\sqrt[4]{T_0^4 + \beta_2^2 z^2}} \exp\Big(\frac{i}{2} \arctan(\frac{\beta_2 z}{T_0^2})\Big) \exp\Big(-\frac{T^2(T_0^2 + i\beta_2 z)}{2(T_0^4 + \beta_2^2 z^2)}\Big), \\ &= \frac{A_0 T_0}{\sqrt[4]{T_0^4 + \beta_2^2 z^2}} \exp\Big[-\frac{T^2 T_0^2}{2(T_0^4 + \beta_2^2 z^2)} + \frac{i}{2}\Big(\arctan(\frac{\beta_2 z}{T_0^2}) - \frac{T^2 \beta_2 z}{(T_0^4 + \beta_2^2 z^2)}\Big)\Big], \\ &= \frac{A_0 T_0}{\sqrt[4]{T_0^4 + \beta_2^2 z^2}} \exp\Big(-\frac{T^2 T_0^2}{2(T_0^4 + \beta_2^2 z^2)}\Big) \exp\Big[\frac{i}{2}\Big(\arctan(\frac{\beta_2 z}{T_0^2}) - \frac{T^2 \beta_2 z}{(T_0^4 + \beta_2^2 z^2)}\Big)\Big]. \end{aligned} \tag{2.30}$$

Thus the amplitude of the Gaussian pulse at any point z along the fiber is given by

$$A(z,T) = \frac{A_0 T_0}{\sqrt[4]{T_0^4 + \beta_2^2 z^2}} \exp\Big(- \frac{T^2 T_0^2}{2(T_0^4 + \beta_2^2 z^2)}\Big) \exp\left[\frac{i}{2}\Big(\arctan(\frac{\beta_2 z}{T_0^2}) - \frac{T^2 \beta_2 z}{(T_0^4 + \beta_2^2 z^2)}\Big)\right]. \tag{2.31}$$

Eq. (2.31) can be further simplified by normalizing quantities:

$$A(z,T) = \frac{A_0}{\sqrt[4]{1 + \beta_2^2 z^2 / T_0^4}} \exp\Big(- \frac{T^2}{2T_0^2(1 + \beta_2^2 z^2/T_0^4)}\Big) \exp\left[\frac{i}{2}\Big(\arctan(\frac{\beta_2 z}{T_0^2}) - \frac{T^2(\beta_2 z/T_0^2)}{T_0^2(1 + \beta_2^2 z^2/T_0^4)}\Big)\right]. \tag{2.32}$$

Comparing Eq (2.19) and (2.32), new pulse width $T_1(z)$ can be obtained:

$$\begin{aligned} T_1(z)^2 &= T_0^2(1 + \beta_2^2 z^2/T_0^4), \\ &= T_0^2(1 + \frac{z^2}{T_0^4/\beta_2^2}), \\ &= T_0^2\Big(1 + (\frac{z}{T_0^2/\beta_2})^2\Big), \\ &= T_0^2\Big(1 + (\frac{z}{L_D})^2\Big), \end{aligned} \tag{2.33}$$

where $L_D = T_0^2 / |\beta_2|$ is the dispersion length in terms of GVD parameter, β_2. The dispersion-broadened pulse width $T_1(z)$ is given by

$$T_1(z) = T_0\sqrt{\Big(1 + (\frac{z}{L_D})^2\Big)}. \tag{2.34}$$

The final expression for the amplitude of the Gaussian pulse at any point z along the fiber yields:

$$A(z,T) = \frac{A_0}{\sqrt[4]{1+(z/L_D)^2}} \exp\Big(-\frac{T^2}{2T_1^2}\Big) \exp\left[\frac{i}{2}\Big(\arctan(\frac{sgn(\beta_2)z}{L_D}) - \frac{T^2(sgn(\beta_2)z/L_D)}{T_1^2}\Big)\right],$$

$$= A_1 A_2 \exp(i\phi_1 + i\phi_2). \tag{2.35}$$

where $A_1 = \frac{A_0}{\sqrt[4]{1+(z/L_D)^2}}$,
$A_2 = \exp\Big(-\frac{T^2}{2T_1^2}\Big) = \exp\Big(-\frac{T^2}{2T_0^2\Big(1+(\frac{z}{L_D})^2\Big)}\Big)$,
$\phi_1 = \frac{1}{2}\arctan(\frac{sgn(\beta_2)z}{L_D})$,
$\phi_2 = -\frac{T^2(sgn(\beta_2)z/L_D)}{2T_1^2} = -\frac{T^2(sgn(\beta_2)z/L_D)}{2T_0^2\Big(1+(\frac{z}{L_D})^2\Big)}$.

According to a book on nonlinear fiber optics [2], expressions for amplitude of a Gaussian pulse at any point z derived in this paper are identical and plots drawn match the characteristics. This gives a notion that formulas and concepts used are correct and leaves a positive note for the rest of the paper.

From the above Eq (2.35), we can observe that the shape of the Gaussian pulse remains the same as it propagates along the fiber, but the width of the pulse is altered by the broadening factor of $\sqrt{1+(z/L_D)^2}$. When $z/L_D = 2$, broadening factor is $\sqrt{5}$, and when $z/L_D = 4$, broadening factor is $\sqrt{17}$ and case for $z/L_D = 0$ is taken as a ideal curve as shown in the Figure (2.1).

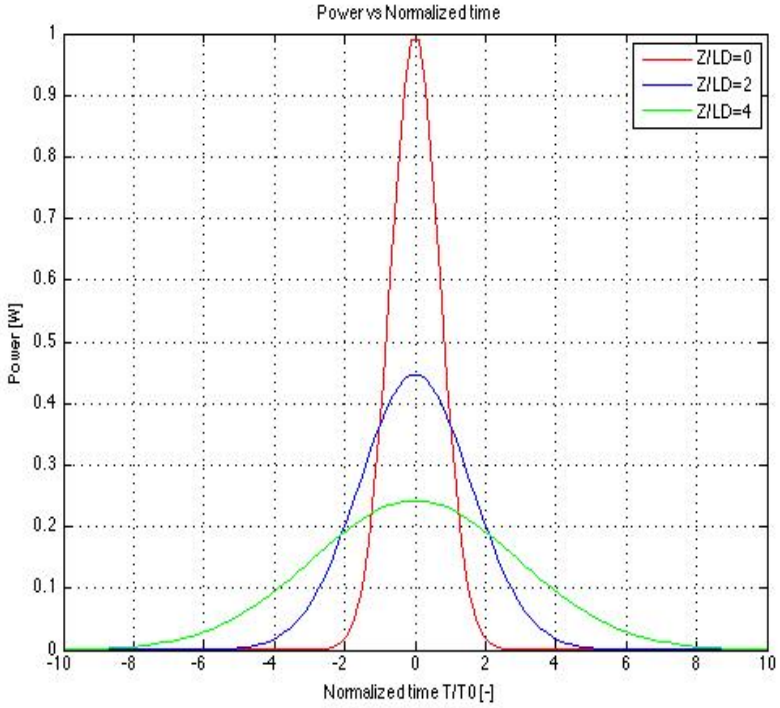

Figure 2.1: Plot of power vs normalized time T/T_0 of a Gaussian pulse for different values of z/L_D

As we know, Power can be expressed as follows

$$\begin{aligned} P &= |A|^2, \\ A &= \sqrt{P} exp(i\phi_A), \\ A(z,T) &= |A(z,T)| \exp(i\phi_A), \\ \phi_A &= Arg(A). \end{aligned} \tag{2.36}$$

Using Eq (2.35), the phase of the signal pulse is given by

$$\begin{aligned} \phi_A &= \phi_1 + \phi_2, \\ &= \frac{1}{2}\arctan\left(\frac{sgn(\beta_2)z}{L_D}\right) - \frac{T^2(sgn(\beta_2)z/L_D)}{2T_0^2\left(1+(\frac{z}{L_D})^2\right)}. \end{aligned} \tag{2.37}$$

The magnitude of the amplitude of pulse envelope is given by

$$A(z,T) = \frac{A_0}{\sqrt[4]{1+(z/L_D)^2}} \exp\Big(-\frac{T^2}{2T_0^2\Big(1+(\frac{z}{L_D})^2\Big)}\Big), \tag{2.38}$$

and the power is given by

$$P(z,T) = \frac{A_0^2}{\sqrt{1+(z/L_D)^2}} \exp\Big(-\frac{T^2}{T_0^2\Big(1+(\frac{z}{L_D})^2\Big)}\Big), \tag{2.39}$$

From the above Eq (2.38) and Eq (2.39), we can observe that shape of Gaussian pulse remains same but the temporal phase of the signal pulse is varied by the GVD parameter and factor z/L_D as shown in the Figure (2.2). Note that as normalized distance z/L_D increases, the peak-to-valley phase variation also increases.
Moreover, as optical power spreads in time, the outer reaches of the temporal phase are invaded. This increases the effective peak-to-valley phase variation.

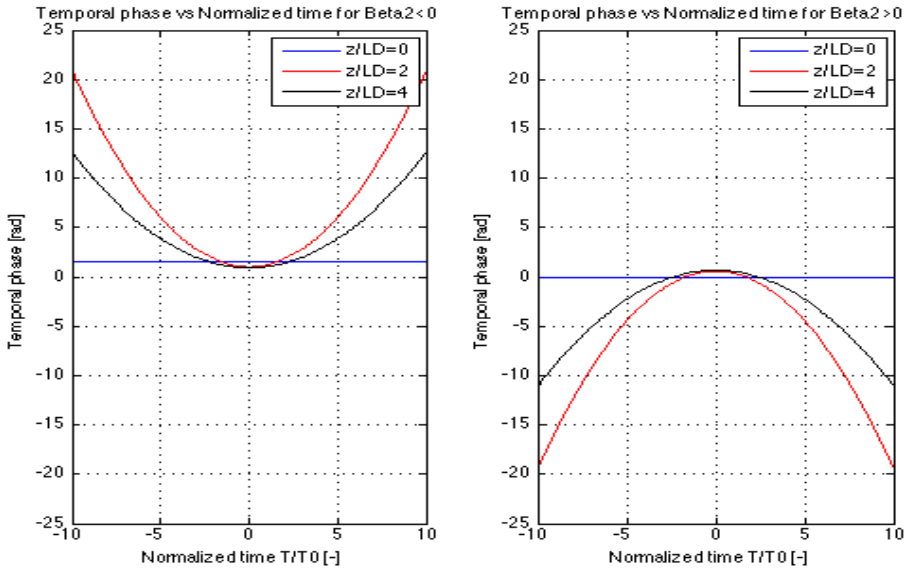

Figure 2.2: Plot of Temporal vs Normalized time T/To of a Gaussian pulse for different values of Z/LD and sign of β_2

A_1 is a constant scaling of the amplitude over T, and A_2 represents the broadening of the pulse with distance and β_2 as shown in the Figure (2.3). ϕ_1 is a constant phase offset over T, while ϕ_2 represents a phase offset variation over T. As such, ϕ_1 does not vary the peak-to-valley voltage range of the phase, and does not contribute to chirp.

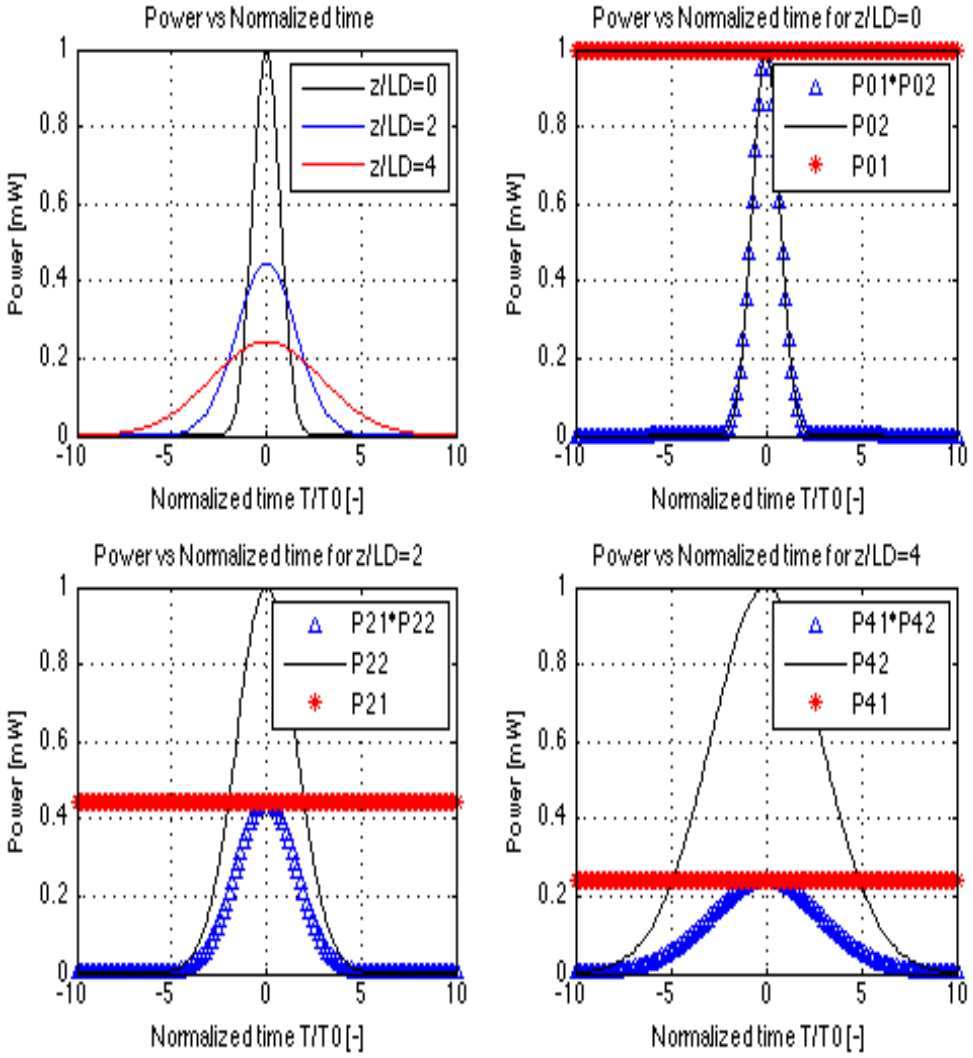

Figure 2.3: Effect of A1 and A2 on power plots of a Gaussian pulse

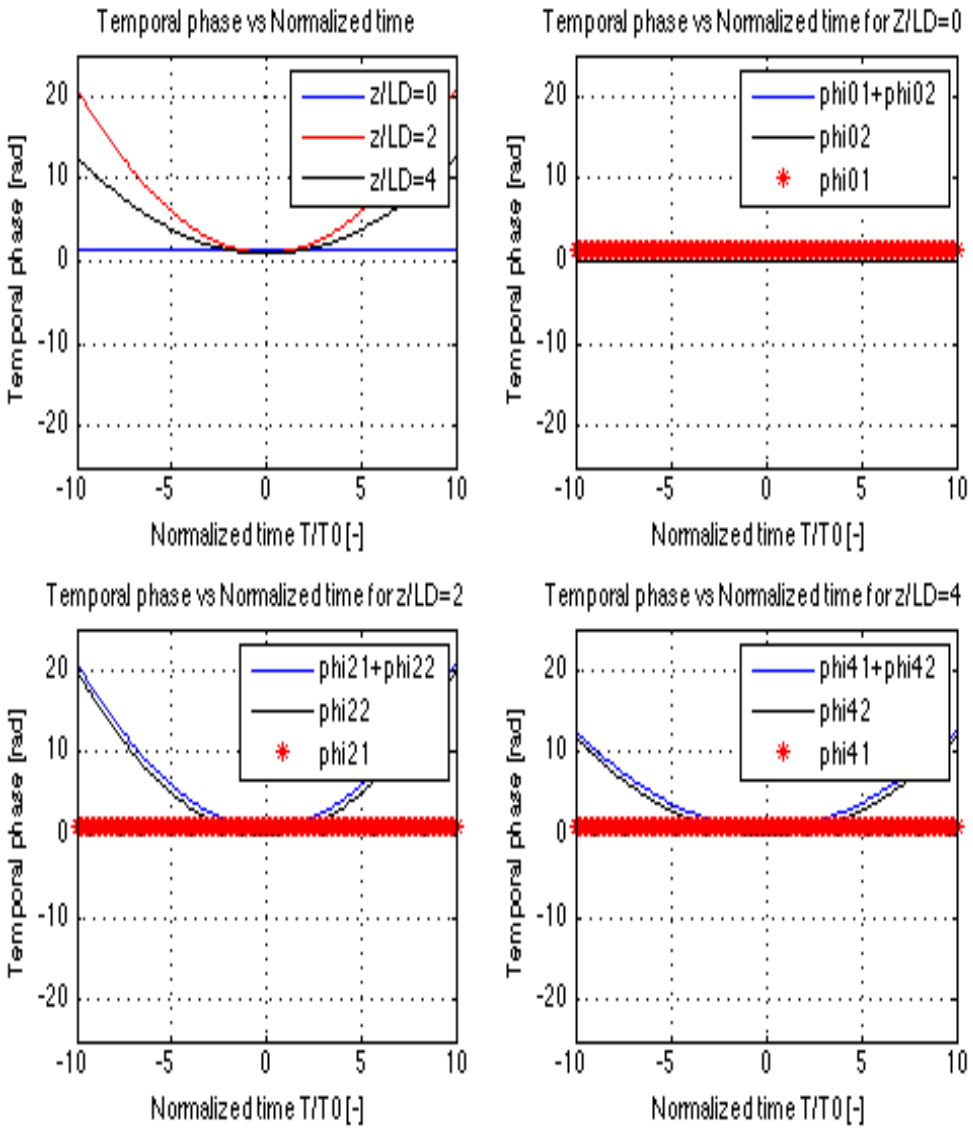

Figure 2.4: Effect of $\phi 1$ and $\phi 2$ on temporal phase plots of a Gaussian pulse for $sgn(\beta_2) < 0$

2.4.2 Numerical Analysis

Using Eq. (2.19), Power of a gaussian pulse at $z = 0$ is shown in the Figure (2.5).

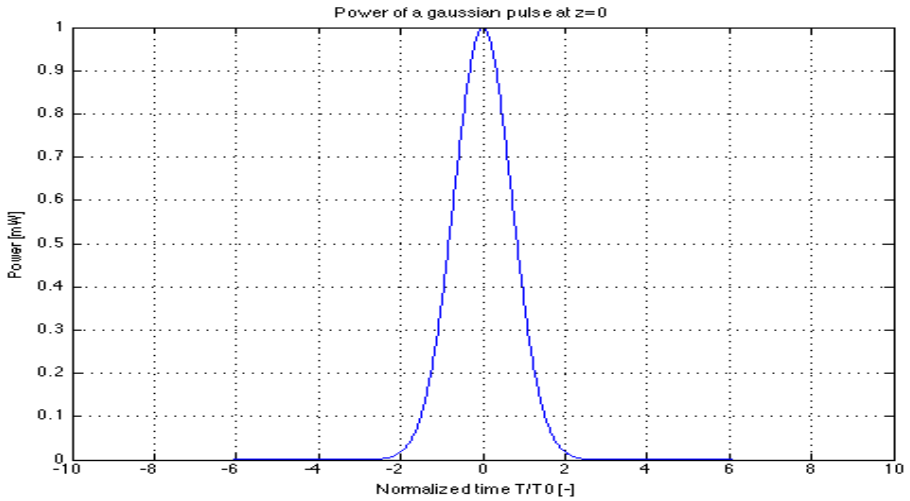

Figure 2.5: Power of a gaussian pulse at $z = 0$

Now, using FFT function in Matlab, FFT of initial power of a optical pulse is shown in the Figure (2.6).

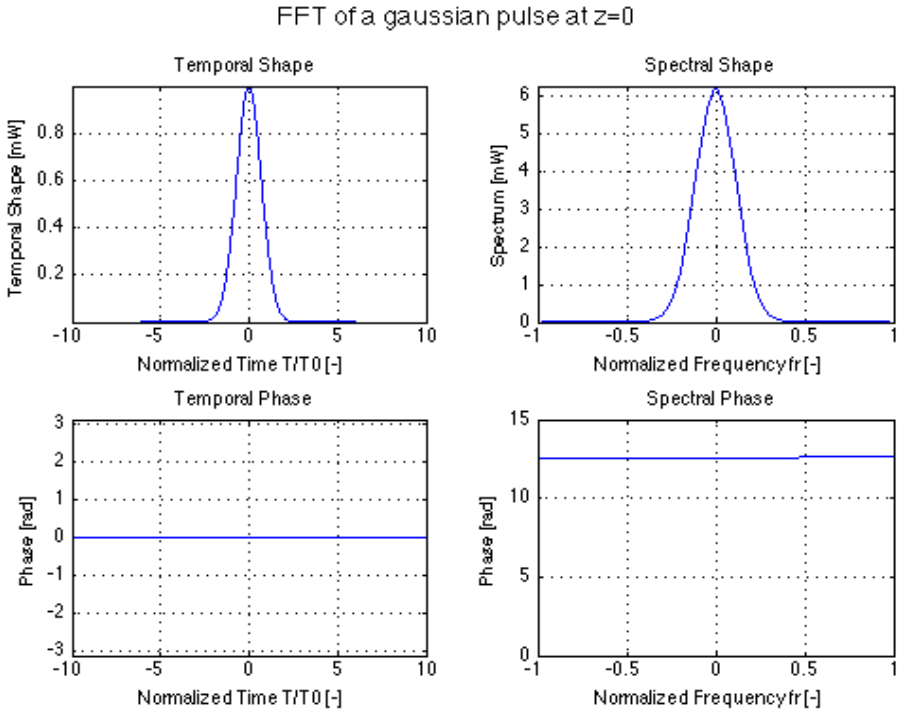

Figure 2.6: Power of a gaussian pulse in frequency domain at $z = 0$

Relation between time and frequency domain

In the above plots, power of a gaussian pulse is plotted against normalized time $\frac{T}{T_0}$, due to which, to obtain the power of a gaussian pulse at $z = \frac{L}{LD}$ in frequency domain, frequency needs to be normalized as well. Normalized frequency fr provided by the FFT is given by

$$\begin{aligned} t &\rightarrow f \\ \frac{t}{T_0} &\rightarrow fT_0 \\ fr &= fT_0 \end{aligned} \tag{2.40}$$

Contribution term

Using Eq.(2.33) and Eq.(2.40), transfer function can be written as:

$$\begin{aligned} H &= \exp(\frac{i}{2}\beta_2\omega^2 z), \\ &= \exp(\frac{i}{2}\beta_2(2\pi f)^2 z), \\ &= \exp(\frac{i}{2}\beta_2(2\pi\frac{fT_0}{T_0})^2 z), \\ &= \exp(\frac{i}{2}\beta_2(2\pi\frac{fr}{T_0})^2 z), \\ &= \exp(\frac{i}{2}\beta_2\frac{(2\pi fr)^2}{T_0^2} z), \\ &= \exp(\frac{i}{2}sgn(\beta_2)(2\pi f)^2\frac{z}{L_D}). \end{aligned} \tag{2.41}$$

where $\omega = 2\pi f$, $sgn(\beta 2)$ is the sign of a GVD parameter and $\frac{z}{L_D}$ is the normalized length of an optical fiber. Thus, normalized frequency term plays a major contribution in modeling the amount of linear dispersion in the optical fiber, given by the transfer function $H(\omega)$.

Using Eq.(2.18) and Eq. (2.41), Electric field of a gaussian pulse at length z of an optical fiber in frequency domain, $E(z, \omega)$ is given by

$$E(z,\omega) = E(0,\omega)\exp(\frac{i}{2}\beta_2\omega^2 z),$$
$$E(z,\omega) = E(0,\omega)\exp(\frac{i}{2}sgn(\beta_2)(2\pi f)^2\frac{z}{L_D}). \tag{2.42}$$

and in time domain, $E((z,T)$ is given by the IFFT of $E(z,\omega)$. Now, plots for Power of a gaussian pulse for each value of normalized length of an optical fiber $\frac{z}{L_D}$ are shown in the figures below:

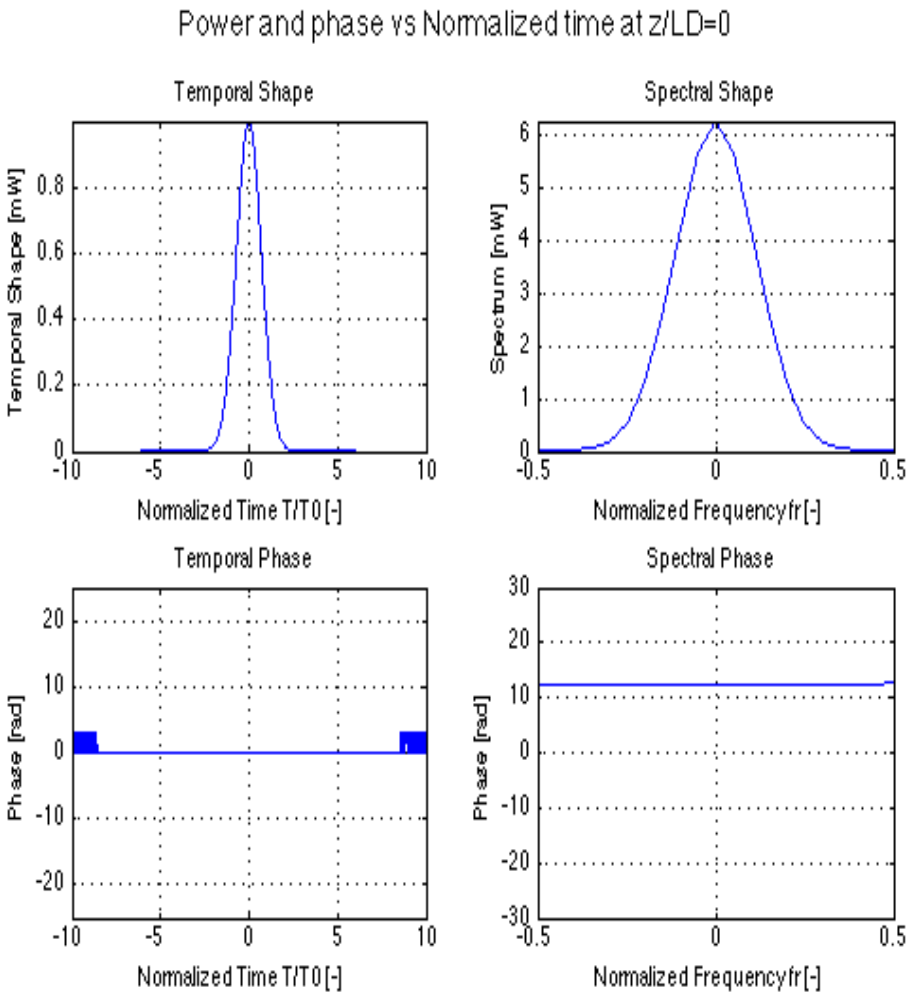

Figure 2.7: Power and phase of a gaussian pulse at $\frac{z}{L_D} = 0$

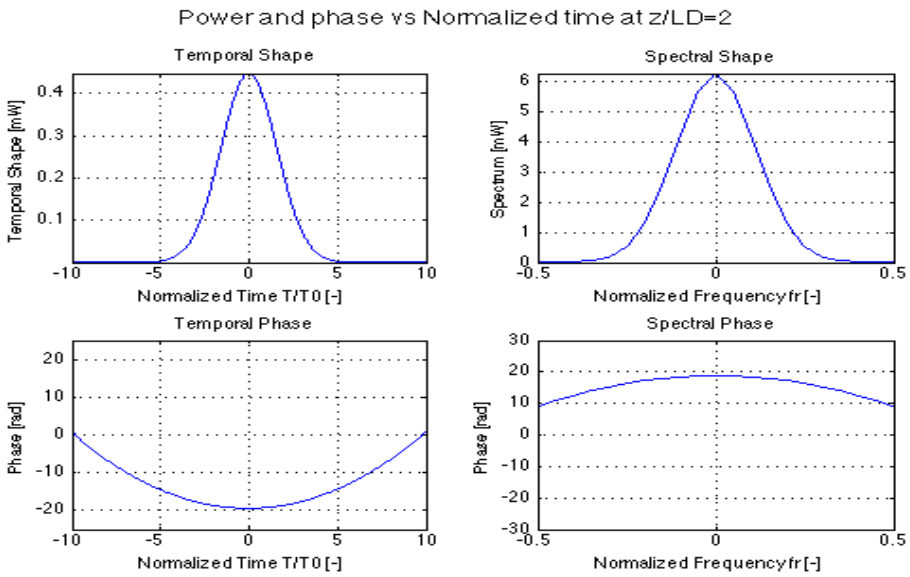

Figure 2.8: Power and phase of a gaussian pulse at $\frac{z}{L_D} = 2$

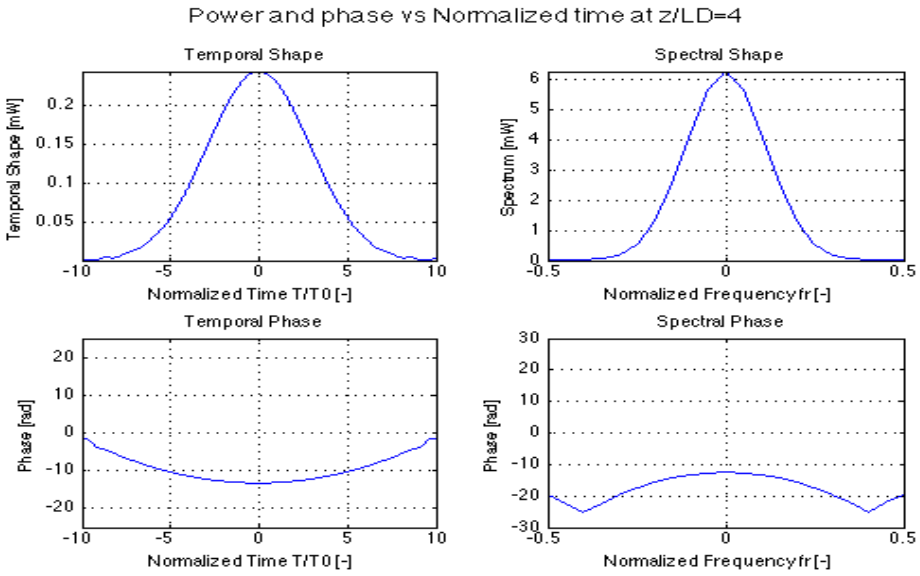

Figure 2.9: Power and phase of a gaussian pulse at $\frac{z}{L_D} = 4$

From the observations of the Figures (2.4),(2.5) and (2.6), Power and phase of a gaussian pulse for different values of $\frac{z}{L_D}$ is shown in the Figure (2.7) and (2.8).

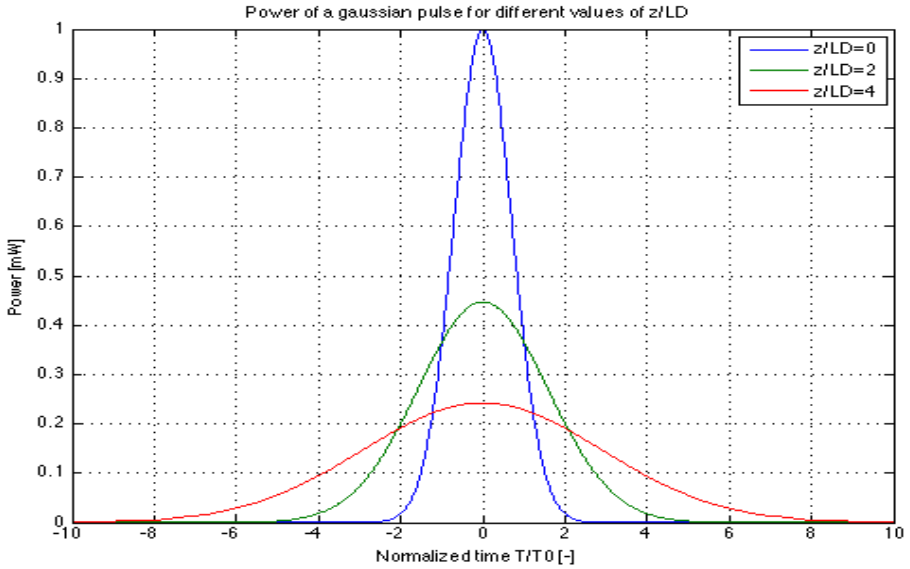

Figure 2.10: Power of a gaussian pulse for different values of $\frac{z}{L_D}$

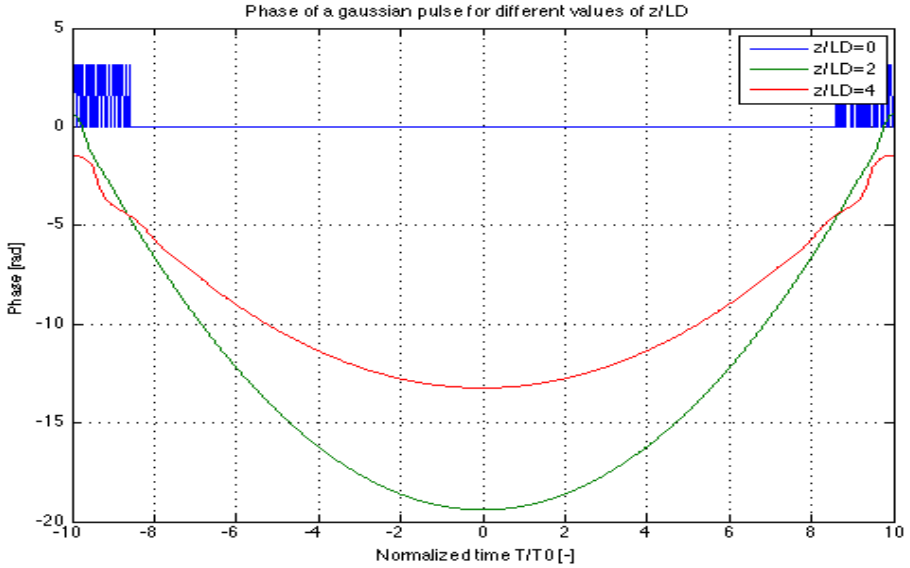

Figure 2.11: Phase of a gaussian pulse for different values of $\frac{z}{L_D}$

Comparing the plots obtained in the analytical and numerical analysis of a gaussian pulse for different values of normalized length $\frac{L}{L_D}$, there is difference of phase offset in the phase plots, but there is no difference for the power plots. Thus, we can say, shape of the pulses obtained in both the analysis for the forward propagation are accurate and can continue to look forward for inverse propagation in the next chapter.

Chapter 3

Inverse-Propagation Model

The focus of my thesis is to compensate transmission impairments in an optical fiber in the electrical domain rather than the optical domain because of flexibility, reproducibility, cost of research, and complexity. To achieve this compensation, we have used a novel dispersion pre-distortion technique to mitigate the chromatic dispersion in an optical fiber in a linear dispersive medium. The idea behind the pre-distortion technique is to generate a pre-compensated optical signal with controlled amplitude and phase at the transmitter. During the transmission, chromatic dispersion in an optical fiber reverses the effect of the pre-compensation so that the desired optical signal is received at the receiver.

3.1 Backward propagation

1. **Define P(L,T)**

The basic method for creating a pre-distorted signal is as follows:
Let P(L,T) be the optimal received power and $\tilde{E}(L,T)$ be the desired optical signal at the receiver. The relation between P(L,T) and $\tilde{E}(L,T)$ is given by

$$P(L,T) = |\tilde{E}(L,T)|^2, \tag{3.1}$$

$$\tilde{E(L,T)} = \sqrt{P(L,T)}exp(i\phi(L,T)). \tag{3.2}$$

The photo-diode at the receiver will measure P(L,T), but $\phi(L,T)$ also exists.

2. **Calculate** $\tilde{E}(L,\omega)$

If $\tilde{E}(L,\omega)$ is the Fourier transform of $\tilde{E}(L,T)$, it can be written as:

$$\begin{aligned}\tilde{E}(L,\omega) &= \mathcal{F}\{\tilde{E}(L,T)\},\\ &= \int_{-\infty}^{\infty} \tilde{E}(L,T)\exp(-i\omega T)\,dT,\\ &= \int_{-\infty}^{\infty} \sqrt{P(L,T)}exp(i\phi(L,T))\exp(-i\omega T)\,dT.\end{aligned} \tag{3.3}$$

3. **Calculate** $\tilde{E_{dc}}(0,\omega)$ **using** $H(\omega)$

Let $\tilde{E_{dc}}(0,\omega)$ be the pre-distortion signal in the frequency domain at the transmitter and it is defined as a product of the desired optical signal in frequency domain at the receiver and inverse transform of the transfer function modeled by chromatic dispersion in an optical fiber given by $H(\omega) = \exp(\frac{i}{2}\beta_2\omega^2 L)$. Using Eq (3.3), $\tilde{E_{dc}}(0,\omega)$ can be written as:

$$\begin{aligned}\tilde{E_{dc}}(0,\omega) &= \tilde{E}(L,\omega)H^{-1}(\omega),\\ &= \tilde{E}(L,\omega)\exp(-\frac{i}{2}\beta_2\omega^2 L),\\ &= \int_{-\infty}^{\infty} \sqrt{P(L,T)}exp(i\phi(L,T))\exp(i\omega T)\,dT\exp(-\frac{i}{2}\beta_2\omega^2 L).\end{aligned} \tag{3.4}$$

4. **Calculate** $\tilde{E_{dc}}(0,T)$ **via inverse Fourier Transform**

Let $\tilde{E_{dc}}(0,T)$ be the pre-distortion signal in the time domain at the transmitter. It is obtained by applying inverse Fourier Transform to the Eq (3.4):

$$
\begin{aligned}
\tilde{E_{dc}}(0,T) &= \mathcal{F}^{-1}\{\tilde{E_{dc}}(0,\omega)\} \\
&= \mathcal{F}^{-1}\{\tilde{E}(L,\omega)H^{-1}(\omega)\}, \\
&= \mathcal{F}^{-1}\{\tilde{E}(L,\omega)\exp(-\frac{i}{2}\beta_2\omega^2 L)\}, \\
&= \frac{1}{2\pi}\int_{-\infty}^{\infty}\int_{-\infty}^{\infty}\sqrt{P(L,T)}exp(i\phi(L,T))\exp(i\omega T)\,dT\exp(-\frac{i}{2}\beta_2\omega^2 L)\exp(-i\omega T)\,d\omega.
\end{aligned}
\tag{3.5}
$$

5. **Cross-check**

As the signal propagates along the fiber, it experiences chromatic dispersion modeled by the transfer function and received optical signal at the receiver is given by $\tilde{E'}(L,T)$.

$$
\begin{aligned}
\tilde{E'}(L,\omega) &= \tilde{E_{dc}}(0,\omega)H(\omega), \\
&= \tilde{E}(L,\omega)H^{-1}(\omega)H(\omega), \\
&= \tilde{E}(L,\omega)\exp(-\frac{i}{2}\beta_2\omega^2 z)\exp(\frac{i}{2}\beta_2\omega^2 z), \\
&= \tilde{E}(L,\omega).
\end{aligned}
\tag{3.6}
$$

Also,

$$
\begin{aligned}
\tilde{E'}(L,T) &= \mathcal{F}^{-1}\{\tilde{E'}(L,\omega)\}, \\
&= \mathcal{F}^{-1}\{\tilde{E}(L,\omega)\}, \\
&= \tilde{E}(L,T).
\end{aligned}
\tag{3.7}
$$

Therefore, the received optical signal at the receiver corresponds to the desired optical signal $\tilde{E}(L,T)$.

6. Calculate $P_{dc}(0,T)$, $\phi_{dc}(0,T)$

Using Eq (3.2), and (3.5), Pre-compensated power of a signal $P_{dc}(0,T)$ can be written as:

$$\begin{aligned}
P_{dc}(0,T) &= |\tilde{E_{dc}}(0,T)|^2, \\
&= |\mathcal{F}^{-1}\{\tilde{E_{dc}}(0,\omega)\}|^2, \\
&= |\mathcal{F}^{-1}\{\int_{-\infty}^{\infty} \sqrt{P(L,T)} exp(i\phi(L,T)) \exp(i\omega T)\, dT \exp(-\frac{i}{2}\beta_2\omega^2 L)\}|^2, \\
&= |\frac{1}{2\pi}\int_{-\infty}^{\infty}\int_{-\infty}^{\infty} \sqrt{P(L,T)} exp(i\phi(L,T)) \exp(i\omega T)\, dT \exp(-\frac{i}{2}\beta_2\omega^2 L) \exp(-i\omega T)\, d\omega|^2,
\end{aligned} \tag{3.8}$$

and Pre-compensated phase of a signal $P_{dc}(0,T)$ $\phi_{dc}(0,T)$ is given by

$$\begin{aligned}
\phi_{dc}(0,T) &= Arg\{\tilde{E_{dc}}(0,T)\}, \\
&= Arg\{\mathcal{F}^{-1}\{\tilde{E_{dc}}(0,\omega)\}\}, \\
&= Arg\{\mathcal{F}^{-1}\{\int_{-\infty}^{\infty} \sqrt{P(L,T)} exp(i\phi(L,T)) \exp(i\omega T)\, dT \exp(-\frac{i}{2}\beta_2\omega^2 L)\}\}, \\
&= Arg\{\frac{1}{2\pi}\int_{-\infty}^{\infty}\int_{-\infty}^{\infty} \sqrt{P(L,T)} exp(i\phi(L,T)) \exp(i\omega T)\, dT \exp(-\frac{i}{2}\beta_2\omega^2 L) \exp(-i\omega T)\, d\omega\}
\end{aligned} \tag{3.9}$$

Once we obtain $P_{dc}(0,T)$, and $\phi_{dc}(0,T)$, we can assess how these quantities depend upon the chromatic dispersion and length of the optical fiber.

3.2 Analysis

3.2.1 Analytical Analysis

Let's take a Gaussian pulse as an example to describe the method of inverse-propagation. The above discussed quantities can be calculated as follows:

1. **Define** $\tilde{E}(L,T)$

Let $\tilde{E}(L,T) = A_0 \exp(-\frac{T^2}{2T_0^2})$ be the desired optical signal at the receiver as shown in the Figure (3.1).

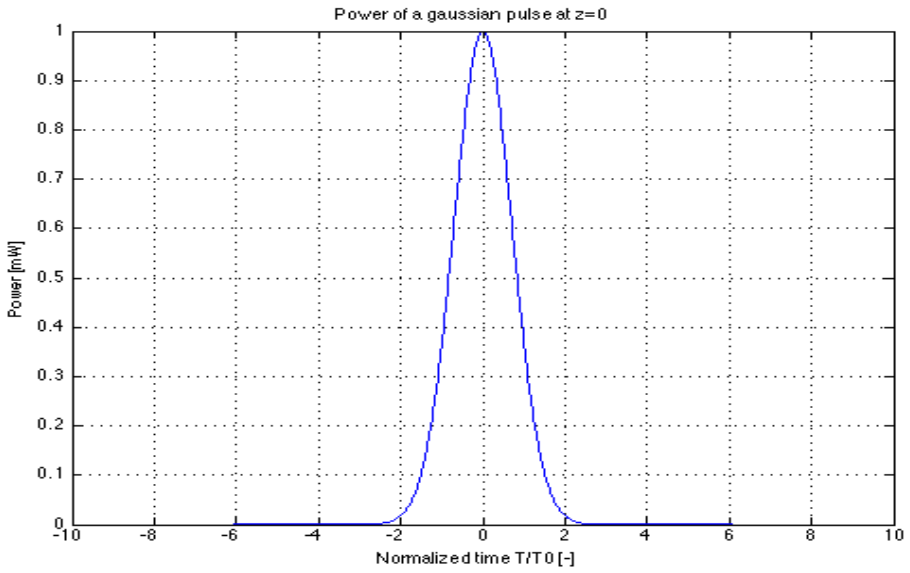

Figure 3.1: Plot of Optimal received power vs Normalized time $\frac{T}{T_0}$

2. **Calculate** $\tilde{E}(L,\omega)$:

Using Eq(2.12), the Fourier transform of $\tilde{E}(L,T)$ yields:

$$\begin{aligned} \tilde{E}(L,\omega) &= \int_{-\infty}^{\infty} \tilde{E}(L,T) \exp(i\omega T)\, dT, \\ &= \int_{-\infty}^{\infty} A_0 \exp(-\frac{T^2}{2T_0^2} + i\omega T). \end{aligned} \tag{3.10}$$

Using the formulae of Fourier Transforms,

$$\int_{-\infty}^{\infty} \exp(-ax^2 + bx)dx = \sqrt{\frac{\pi}{a}} \exp(\frac{b^2}{4a}). \tag{3.11}$$

Here $a = \frac{1}{2T_0^2}$ and $b = i\omega$, then Eq (3.10) yields:

$$\tilde{E}(L, \omega) = A_0 T_0 \sqrt{2\pi} \exp(-\frac{\omega^2 T_0^2}{2}). \tag{3.12}$$

3.**Calculate $\tilde{E_{dc}}(0, \omega)$ using $H(\omega)$**

Using Eq (3.4), $\tilde{E_{dc}}(0, \omega)$ can be written as:

$$\begin{aligned} \tilde{E_{dc}}(0, \omega) &= \tilde{E}(L, \omega).H^{-1}(\omega), \\ &= A_0 T_0 \sqrt{2\pi} \exp(-\frac{\omega^2 T_0^2}{2}) \exp(-\frac{i}{2}\beta_2 \omega^2 L), \\ &= A_0 T_0 \sqrt{2\pi} \exp(-\frac{\omega^2 T_0^2}{2} - \frac{i}{2}\beta_2 \omega^2 L). \end{aligned} \tag{3.13}$$

4.**Calculate $\tilde{E_{dc}}(0, T)$ via inverse Fourier Transform**

Applying the inverse transform to the Eq (3.13) and using Eq (3.11):

$$\begin{aligned} \tilde{E_{dc}}(0, T) &= \mathcal{F}^{-1}\{\tilde{E_{dc}}(0, \omega)\}, \\ &= \mathcal{F}^{-1}\{\tilde{E}(L, \omega) H^{-1}(\omega)\}, \\ &= \mathcal{F}^{-1}\{A_0 T_0 \sqrt{2\pi} \exp\Big(-\frac{\omega^2}{2}(T_0^2 + i\beta_2 L)\Big)\}, \\ &= \frac{1}{2\pi} \int_{-\infty}^{\infty} A_0 T_0 \sqrt{2\pi} \exp\Big(-\frac{\omega^2}{2}(T_0^2 + i\beta_2 L)\Big) \exp(-i\omega T)\, d\omega, \\ &= \frac{1}{2\pi} \int_{-\infty}^{\infty} A_0 T_0 \sqrt{2\pi} \exp\Big(-\frac{\omega^2}{2}(T_0^2 + i\beta_2 L) - \omega T\Big)\, d\omega, \\ &= \frac{A_0 T_0}{\sqrt{T_0^2 + i\beta_2 L}} \exp\big[-\frac{T^2}{2(T_0^2 + i\beta_2 L)}\big]. \end{aligned} \tag{3.14}$$

where $a = (\frac{T_0^2 + i\beta_2 L}{2})$ and $b = -iT$.

Using the same technique employed in Eq (2.28) and (2.29), the final expression

for $\tilde{E_{dc}}(0,T)$ yields:

$$\tilde{E_{dc}}(0,T) = \frac{A_0 T_0}{\sqrt[4]{T_0^4 + \beta_2^2 L^2}} \exp\Big(- \frac{T^2 T_0^2}{2(T_0^4 + \beta_2^2 L^2)}\Big) \exp\left[\frac{i}{2}\Big(\frac{T^2 sgn(\beta_2) L}{(T_0^4 + \beta_2^2 L^2)} - \arctan(\frac{sgn(\beta_2) L}{T_0^2})\Big)\right]. \tag{3.15}$$

Using Eq (2.33) and (2.34), it can be further simplified as:

$$\begin{aligned}\tilde{E_{dc}}(0,T) &= \frac{A_0}{\sqrt[4]{1 + (L/L_D)^2}} \exp\Big(- \frac{T^2}{2T_1^2}\Big) \exp\left[\frac{i}{2}\Big(\frac{T^2 (sgn(\beta_2) L/L_D)}{T_1^2} - \arctan(\frac{sgn(\beta_2) L}{L_D})\Big)\right], \\ &= A_1 A_2 \exp(i\phi_1 + i\phi_2).\end{aligned} \tag{3.16}$$

where $A_1 = \frac{A_0}{\sqrt[4]{1+(L/L_D)^2}}$,

$A_2 = \exp\Big(- \frac{T^2}{2T_1^2}\Big) = \exp\Big(- \frac{T^2}{2T_0^2\Big(1+(\frac{z}{L_D})^2\Big)}\Big)$,

$\phi_1 = -\frac{1}{2}\arctan(\frac{sgn(\beta_2) L}{L_D})$,

$\phi_2 = \frac{T^2 (sgn(\beta_2) L/L_D)}{2T_1^2} = \frac{T^2 (sgn(\beta_2) z/L_D)}{2T_0^2\Big(1+(\frac{z}{L_D})^2\Big)}$.

Power and phase plots of a pre-distorted signal $\tilde{E_{dc}}(0,\omega)$ are shown in the Figure (3.2) and (3.3).

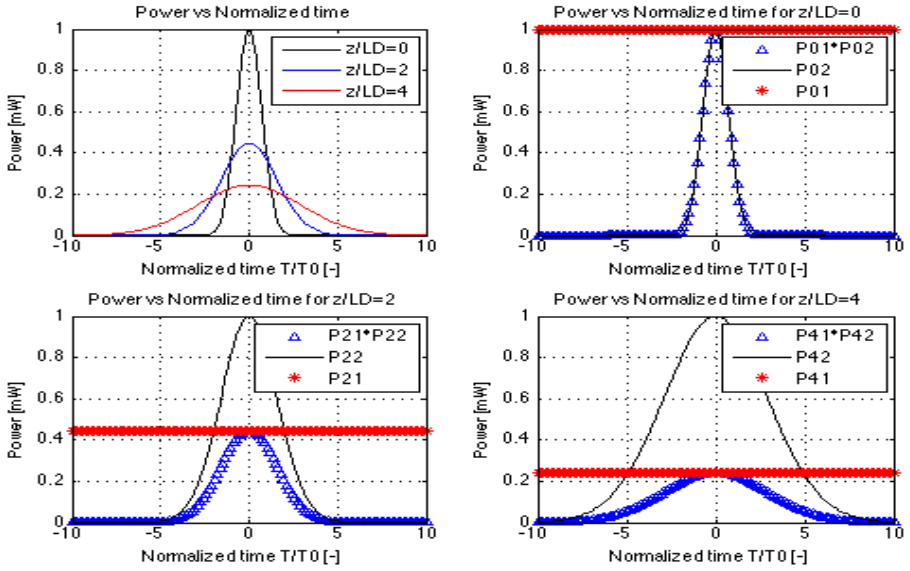

Figure 3.2: Plots for power of pre-distorted signal for different values of $\frac{z}{L_D}$

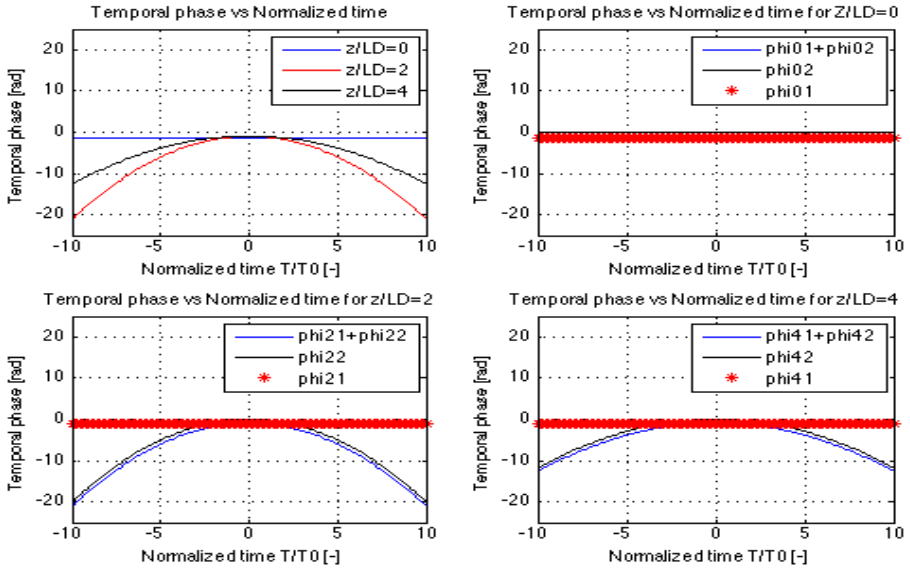

Figure 3.3: Plots of Power and Phase of iFFT'd signal for normalized distance $\frac{z}{L_D}$

Comparing Eq (2.35) and (3.16), analytically, we can conclude Forward-propagation model differs from Inverse-propagation model in terms of sign of phase component ϕ and no difference between the power plots.

5.**Cross-check**

The received optical signal at the receiver $\tilde{E'}(L,T)$ corresponds to the desired optical signal $\tilde{E}(L,T)$. Using Eq (3.7) and (3.11), equation for $\tilde{E'}(L,T)$ yields:

$$\begin{aligned}
\tilde{E'}(L,T) &= \mathcal{F}^{-1}\{\tilde{E'}(L,\omega)\}, \\
&= \mathcal{F}^{-1}\{\tilde{E}(L,\omega)\}, \\
&= \frac{1}{2\pi}\int_{-\infty}^{\infty} T_0\sqrt{2\pi}\exp(-\frac{\omega^2 T_0^2}{2})\exp(-i\omega T)\,d\omega, \\
&= \frac{1}{2\pi}\int_{-\infty}^{\infty} T_0\sqrt{2\pi}\exp(-\frac{\omega^2 T_0^2}{2} - i\omega T), \\
&= \exp(-\frac{T^2}{2T_0^2}), \\
&= \tilde{E}(L,T).
\end{aligned} \tag{3.17}$$

where $a = (\frac{T_0^2}{2})$ and $b = -iT$.

3.2.2 Numerical Analysis

Using Eq. (2.19), Power of a desired optical signal $P(L,T)$ at the receiver is shown in the Figure (3.4).

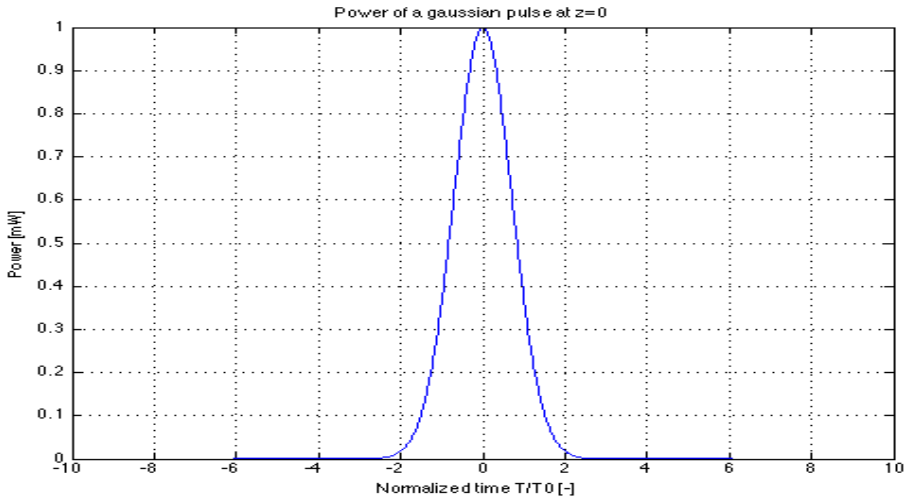

Figure 3.4: Power of a desired optical signal at the receiver

Now, using FFT function in Matlab, FFT of desired power of a optical pulse is shown in the Figure (3.5).

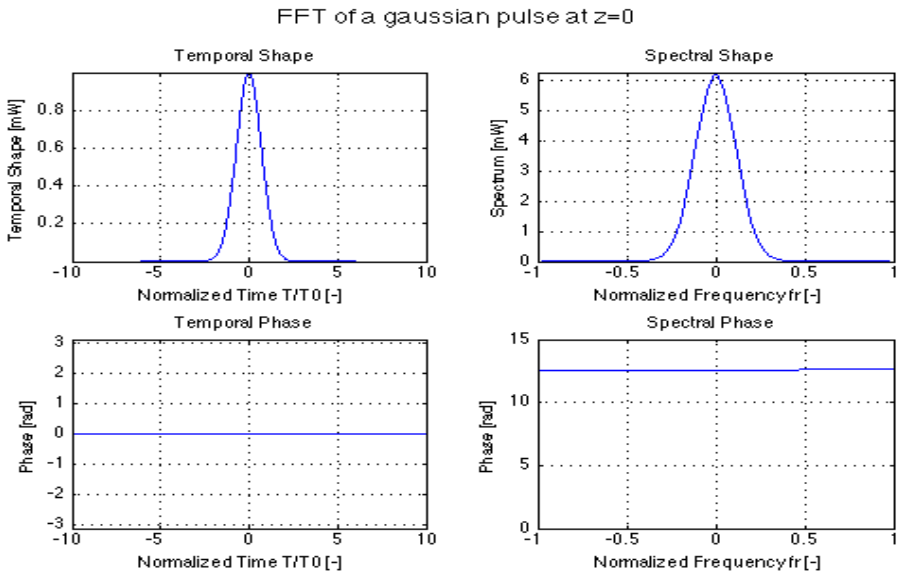

Figure 3.5: FFT of a desired optical signal

Using the relation between time and frequency domain explained in Eq.(3.18) and contribution term in Eq. (3.19), power of a pre-distorted signal in time domain $P_{dc}(0,T)$ for different values of normalized length of optical fiber $\frac{z}{L_D}$ are shown in the figures below.

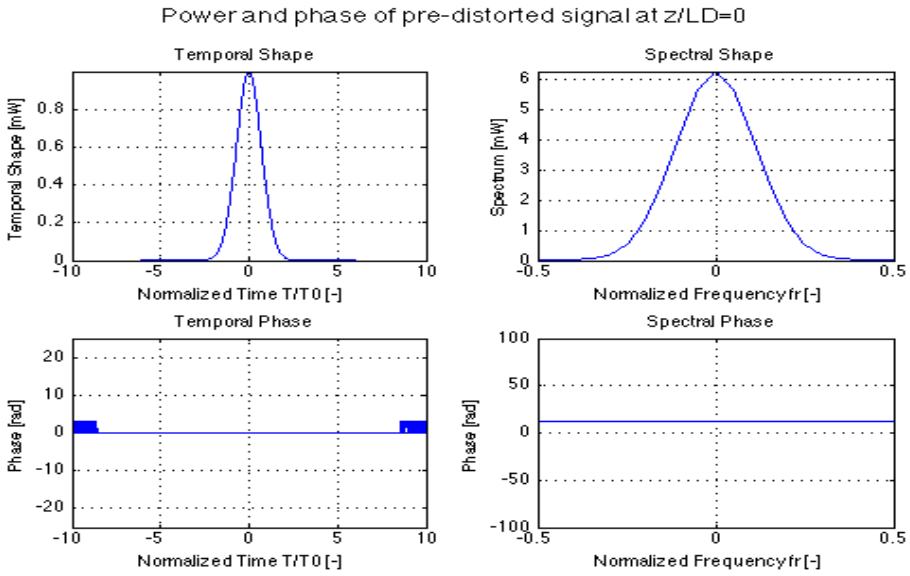

Figure 3.6: Power and phase of a pre-distorted signal $\frac{z}{L_D} = 0$

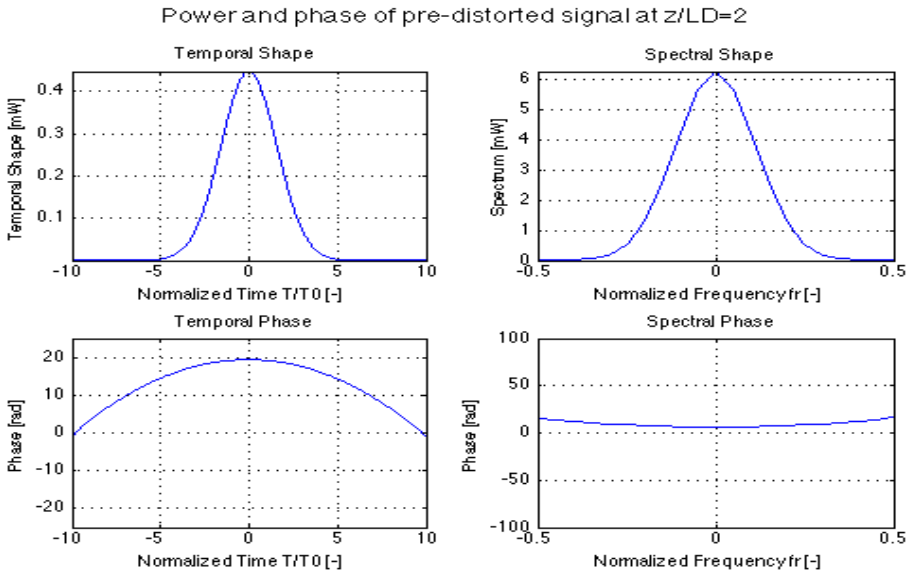

Figure 3.7: Power and phase of a pre-distorted signal $\frac{z}{L_D} = 2$

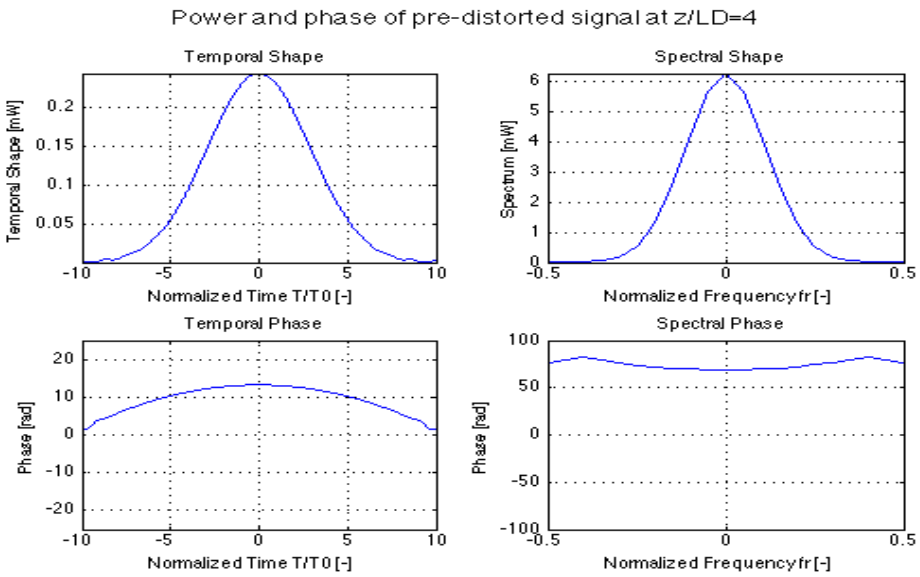

Figure 3.8: Power and phase of a pre-distorted signal $\frac{z}{L_D} = 4$

From the observations of the Figures (3.6),(3.7) and (3.8), power and phase of a pre-distored signal for all values of normalized length of an optical fiber $\frac{z}{L_D}$ are shown in the Figure (3.9) and (3.10).

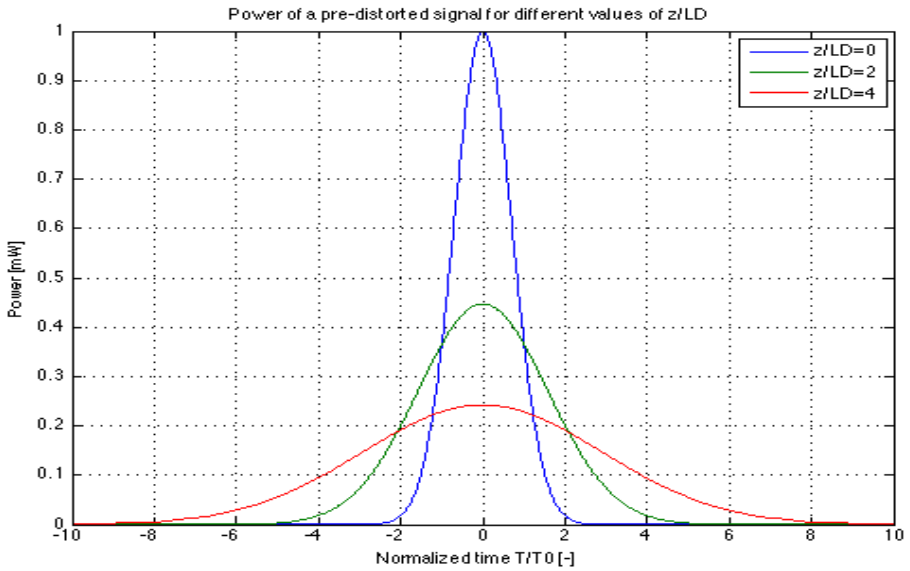

Figure 3.9: Power of a pre-distorted signal for different values of $\frac{z}{L_D}$

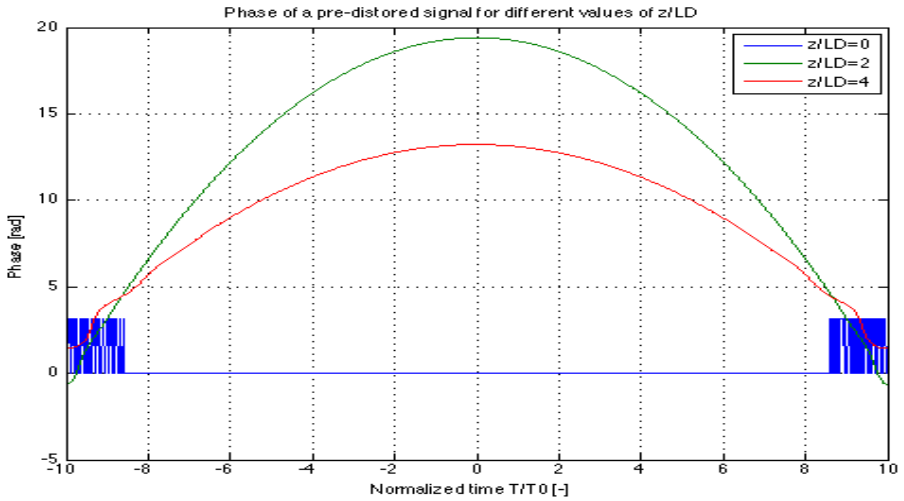

Figure 3.10: Phase of a pre-distorted signal for different values of $\frac{z}{L_D}$

Comparing the plots obtained in the analytical and numerical analysis of a pre-distorted signal for different values of normalized length of an optical fiber $\frac{L}{L_D}$, there is difference of phase offset in the phase plots, but there is no difference for the power plots. Thus, we can say, shape of the pulses obtained in both the analysis for the Inverse propagation are accurate and can continue to look forward to implement the pre-distortion model and investigate the characteristics and parameters used to analyze the signal in both optical and electrical domain.

Sanity-check

Using Eq.(3.17), Power and phase of a received optical signal at the end of an optical fiber for different values of normalized lengths are observed to be same as shown in the Figure (3.11) , that means, we are able to successfully recover the desired signal at the receiver by the means of pre-distortion. Thus, we can say, analysis for the inverse propagation is accurate and can continue to investigate the pre-distortion analysis in the electrical domain using a Dual-drive MZM and digital signal processing to generate a pre-distorted signal and obtain the plots against various characteristics involved in the process.

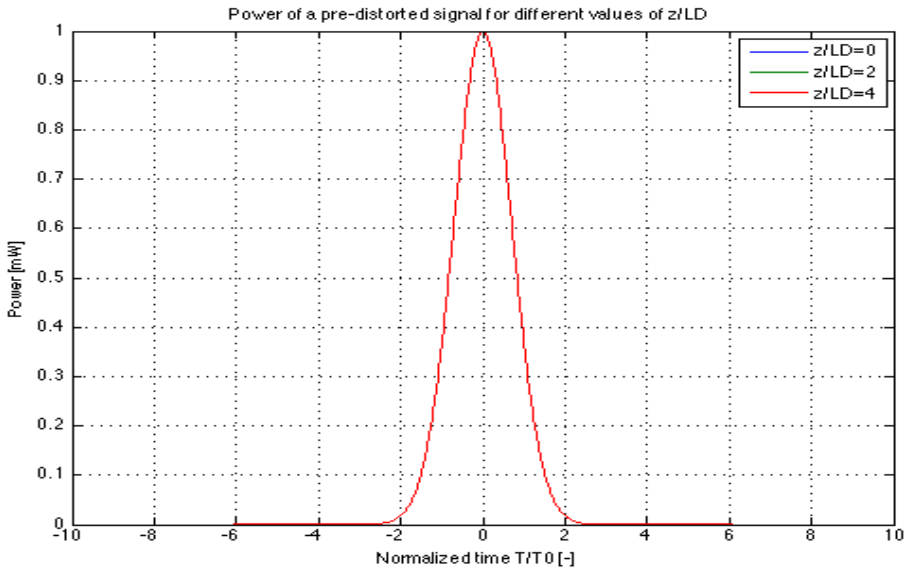

Figure 3.11: Power of a received optical signal for different values of $\frac{z}{L_D}$

Chapter 4

Generation of pre-distorted signals using Dual-Drive Mach Zender Modulator

A Mach-Zehnder modulator(MZM) is an optical device which uses the electro-optic effect to modulate the signals in terms of amplitude, phase, frequency and polarization. The MZM is made of a crystal, such as lithium niobate ($LiNb0_3$), whose refractive index depends upon the strength of electric field. The underlying electro-optic effect is also termed as Pockels effect which is described as a phenomena in which the refractive index of the medium is varied by applying a low-level DC voltage or low-level electric field. A Dual-drive MZM works on the basic operation of a MZM and it's design consists of one broadband RF electrode per arm of an optical interferometer driven by an electrical voltages RF and Vbias as shown in the Figure (4.1). Both RF electrodes are designed in such a way that they are synchronized to modulate the electrical field of a signal at the same time and with the same group delays[5]. Working of a DD-MZM is characterized by applying an electrical voltage that is half the voltage of a single-drive device to each RF port with a phase shift of π between them: $-\frac{V}{2}, +\frac{V}{2}$ and biasing each arm at the bias point, (in this paper, it is $3V\pi/2$) that results in modulation. Thus, by changing the voltages, we can control the overlapping of electric-field in each

arm of an optical interferometer resulting in absence or presence of intensity and phase modulation. In this paper, RF and bias voltage magnitudes are considered to be equal and opposite in direction and this process is adjusted to compensate or enhance the effect of dispersion in an optical fiber.

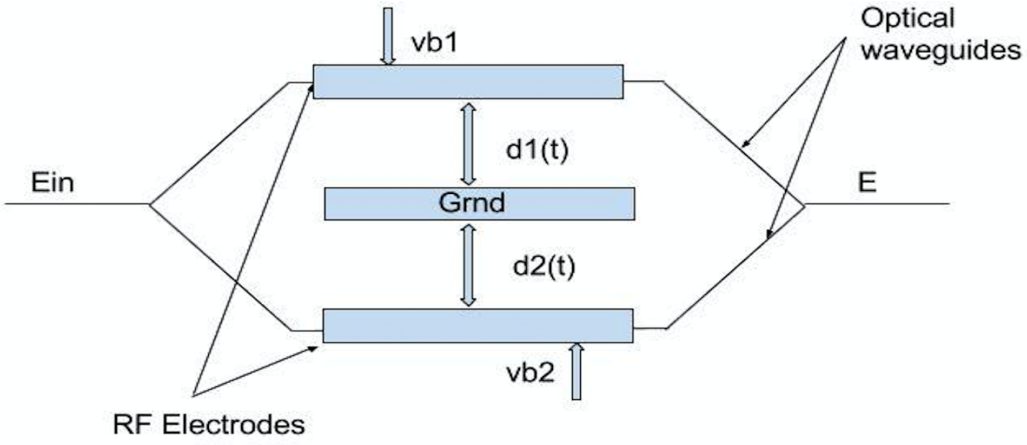

Figure 4.1: Operation of a Dual-drive MZM

4.0.1 Analysis of signal generation using a dual-drive MZM

Let $E_{dc}(0,T)$ be the pre-distorted signal produced by a dual-drive MZM which can be written in the form

$$E_{dc}(0,T) = E_{in}\sin(\phi_1)\exp(i\phi_2), \tag{4.1}$$

where E_{in} is the input electric field produced by a continuous wave laser source, ϕ_1 and ϕ_2 are phase parameters. Using MZM analysis, phase parameters are defined as:

$$
\begin{aligned}
\phi_1 &= \frac{(a1-a2)}{2}, \\
&= -\frac{\pi L}{\lambda_0}\Big[(V_1+V_{b1})\mu_1 - (V_2+V_{b2})\mu_2\Big], \\
&= -\frac{\pi}{2}\Big[\frac{(V_1+V_{b1})}{V_{\pi 1}}\frac{\mu_1}{|\mu_1|} - \frac{(V_2+V_{b2})}{V_{\pi 2}}\frac{\mu_2}{|\mu_2|}\Big], \\
&= -\frac{\pi}{2}\Big[\frac{(V_1+V_{b1})}{V_{\pi 1}}S_1 - \frac{(V_2+V_{b2})}{V_{\pi 2}}S_2\Big], \\
&= -\frac{\pi}{2}\Big[(\nu_1+\nu_{b1})S_1 - \frac{(V_2+V_{b2})}{V_{\pi 2}}S_2\Big],
\end{aligned}
\tag{4.2}
$$

where half-wave voltage parameters are written in the form

$$
V_{\pi 1} = \frac{\lambda_0}{2|\mu_1|L}, \tag{4.3}
$$

and

$$
V_{\pi 2} = \frac{\lambda_0}{2|\mu_2|L}. \tag{4.4}
$$

and $\nu_1 = \frac{V_1}{V_{\pi 1}}$, $\nu_{b1} = \frac{V_{b1}}{V_{\pi 1}}$ and S_1, S_2 are signs of μ_1 and μ_2 respectively.
Now using Eq.(4.3) and Eq.(4.4), let us consider writing V_2 in the form,

$$
\begin{aligned}
\frac{V_2}{V_{\pi 2}} &= \frac{V_2}{V_{\pi 2}}, \\
&= \frac{V_2}{V_{\pi 2}}.\frac{V_{\pi 1}}{V_{\pi 1}}, \\
&= \frac{V_2}{V_{\pi 1}}.\frac{V_{\pi 1}}{V_{\pi 2}}, \\
&= \frac{V_2}{V_{\pi 1}}.\frac{|\mu_2|}{|\mu_1|}, \\
&= \frac{V_2}{V_{\pi 1}}.M, \\
&= \nu_2 M,
\end{aligned}
\tag{4.5}
$$

where M is defined as absolute value of ratio of electro-optic coefficients μ_1 and μ_2: $M = \frac{|\mu_1|}{|\mu_2|}$. Similarly, $\frac{V_{b2}}{V_{\pi 2}} = \nu_{b2} M$.

Thus, using Eq.(4.2) and Eq.(4.5), ϕ_1 is given by,

$$\phi_1 = -\frac{\pi}{2}\Big[(\nu_1 + \nu_{b1})S_1 - (\nu_2 + \nu_{b2})MS_2\Big]. \tag{4.6}$$

In similar fashion, phase parameter ϕ_2 can be written in the form,

$$\begin{aligned} \phi_2 &= \frac{(a1 + a2)}{2} + \frac{\pi}{2}, \\ &= -\frac{\pi}{2}\Big[(\nu_1 + \nu_{b1})S_1 + \frac{(V_2 + V_{b2})}{V_{\pi 2}}S_2 + \frac{\pi}{2}\Big], \\ &= -\frac{\pi}{2}\Big[(\nu_1 + \nu_{b1})S_1 + (\nu_2 + \nu_{b2})MS_2 + \frac{\pi}{2}\Big]. \end{aligned} \tag{4.7}$$

4.0.2 Intrinsic chirp parameter and S_m

Intrinsic chirp parameter of a single drive MZM driven by driving voltages d1 and d2 is given by,

$$\alpha_0 = \frac{\mu_1 + \mu_2}{\mu_1 - \mu_2}. \tag{4.8}$$

Re-ordering the above Eq. (4.8), relation between electro-optic coefficients μ_1 and μ_2, the ratio of μ's can be written in the form,

$$\frac{\mu_2}{\mu_1} = \frac{\alpha_0 - 1}{\alpha_0 + 1}. \tag{4.9}$$

Thus, $M = \frac{|\mu_2|}{|\mu_1|} = \frac{|\alpha_0 - 1|}{|\alpha_0 + 1|}$.

Note that the sign of S_2 can be written as,

$$S_2 = S_1.S_m, \tag{4.10}$$

where $S_m = \text{sgn}(\frac{\mu_2}{\mu_1})$.

But in the case of a dual-drive MZM, typically we consider $\text{sgn}(\mu_1) = \text{sgn}(\mu_2)$ and it is sought that $\mu_1 = \mu_2$, which leads to an infinite intrinsic chirp parameter α_0, hence it is not used a useful quantity in the further analysis. Based on this fact, we can write $M = 1$ and $S_m = 1$, but to understand it's impact on the result, these parameters are not assigned any constant value.

Now using Eq.(4.8) and Eq.(4.10), Eq.(4.2) and Eq.(4.7) can be re-arranged as:

$$\begin{aligned}
\phi_1 &= -\frac{\pi}{2}\Big[(\nu_1 + \nu_{b1})S_1 - (\nu_2 + \nu_{b2})MS_2\Big], \\
&= -\frac{\pi}{2}\Big[(\nu_1 + \nu_{b1})S_1 - (\nu_2 + \nu_{b2})MS_1S_m\Big], \\
&= -\frac{\pi}{2}S_1\Big[(\nu_1 + \nu_{b1}) - (\nu_2 + \nu_{b2})MS_m\Big].
\end{aligned} \tag{4.11}$$

The phase parameter ϕ_2 is given by,

$$\phi_2 = -\frac{\pi}{2}S_1\Big[(\nu_1 + \nu_{b1}) + (\nu_2 + \nu_{b2})MS_m\Big] + \frac{\pi}{2}. \tag{4.12}$$

4.1 Relation between driving voltages V_1 and V_2

Using Eq.(4.1), the power of a pre-distorted signal is given by,

$$\begin{aligned} P_{dc}(0,T) &= |E|^2, \\ &= |E_{in}\sin(\phi_1)\exp(i\phi_2)|^2, \\ &= |E_{in}|^2|\sin(\phi_1)|^2, \\ &= P_{in}\sin^2(\phi_1). \end{aligned} \tag{4.13}$$

where initial power, $P_{in} = |E_{in}|^2$.

Re-arranging above Eq.(4.13), ϕ_1 is written in the form,

$$\begin{aligned} \sin^2(\phi_1) &= \frac{P_{dc}(0,T)}{P_{in}}, \\ \sin(\phi_1) &= \pm\sqrt{\frac{P_{dc}(0,T)}{P_{in}}}, \\ \phi_1 &= \pm\arcsin\Big(\sqrt{\frac{P_{dc}(0,T)}{P_{in}}}\Big), \end{aligned} \tag{4.14}$$

Thus, there is a sign ambiguity in knowing ϕ_1 based on $\sqrt{P}$.

The phase of the signal is given by $\phi(t)$ is equal to ϕ_2.

$$\phi_{dc}(0,T) = \phi_2. \tag{4.15}$$

Using Eq. (4.11) and Eq. (4.12), Eq (4.14) and Eq.(4.15) can be written as,

$$-\frac{\pi}{2}S_1\Big[(\nu_1+\nu_{b1})-(\nu_2+\nu_{b2})\Big] = \pm\arcsin\Big(\sqrt{\frac{P_{dc}(0,T)}{P_{in}}}\Big), \tag{4.16}$$

$$-\frac{\pi}{2}S_1\Big[(\nu_1+\nu_{b1})+(\nu_2+\nu_{b2})\Big]+\frac{\pi}{2}=\phi_{dc}(0,T). \tag{4.17}$$

Driving voltage V_1 is obtained by adding Eq.(4.16) and (4.17),

$$\nu_1=\frac{1}{\pi S_1}\Big[\frac{\pi}{2}-\phi_{dc}(0,T)\mp\arcsin\Big(\sqrt{\frac{P_{dc}(0,T)}{P_{in}}}\Big)\Big]-\nu_{b1}, \tag{4.18}$$

and driving voltage V_2 is obtained by subtracting Eq.(4.16) and (4.17),

$$\begin{aligned}\nu_2&=\frac{1}{\pi M S_1 S_m}\Big[\frac{\pi}{2}-\phi_{dc}(0,T)\pm\arcsin\Big(\sqrt{\frac{P_{dc}(0,T)}{P_{in}}}\Big)\Big]-\nu_{b2},\\&=\frac{1}{\pi M S_2}\Big[\frac{\pi}{2}-\phi_{dc}(0,T)\pm\arcsin\Big(\sqrt{\frac{P_{dc}(0,T)}{P_{in}}}\Big)\Big]-\nu_{b2}.\end{aligned} \tag{4.19}$$

4.2 Analysis

To analyze the importance of driving voltages that are required to generate a pre-distorted signal $E_{dc}(0,T)$, let us consider parameters M, S1 and S2 to be a constant value 1 and biasing voltages to be equal to 0 for initial analysis. Using Eq. (3.16), driving voltages $d_1(t)$ and $d_2(t)$ for different cases of normalized length $\frac{z}{L_D}$ are shown in the Figure (4.2) and (4.3). From the observation of figures listed below, we can say driving voltages $d_1(t)$ and $d_2(t)$ differ by an offset of $\sin^{-1}\Big(\sqrt{\frac{P_{dc}(0,T)}{P_{in}}}\Big)$. For further analysis, driving voltages can be plotted for different values of biasing voltages and electro-optic parameters $\mu 1$ and $\mu 2$.

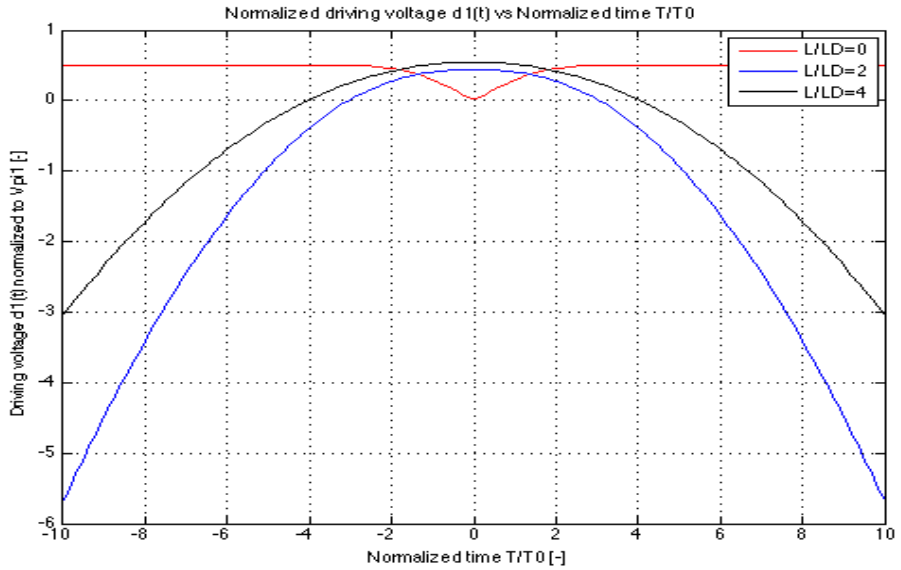

Figure 4.2: Driving voltage $d_1(t)$ for different values of $\frac{z}{L_D}$

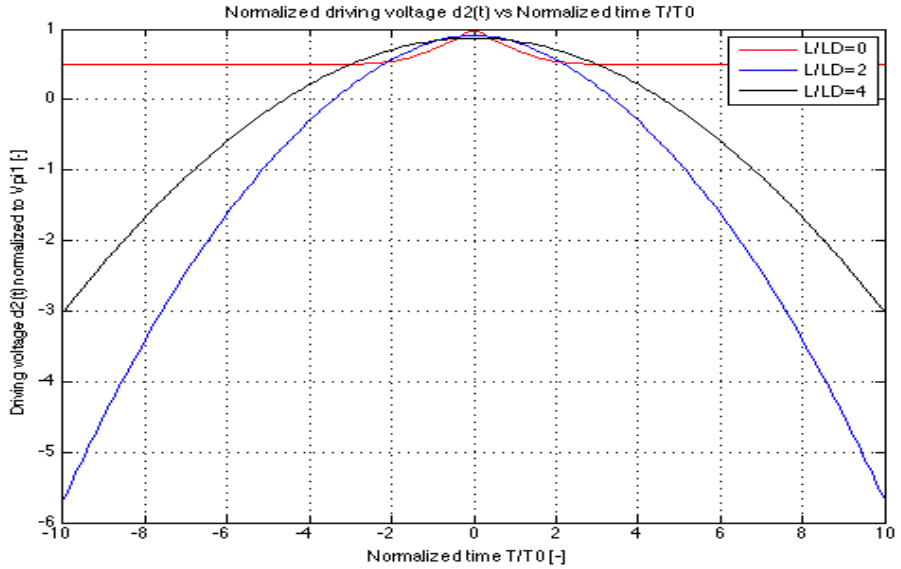

Figure 4.3: Driving voltage $d_2(t)$ for different values of $\frac{z}{L_D}$

Chapter 5

Digital Processor Design

5.1 Introduction

This chapter details the working model of DSP processor design in detail. Processor is implemented to pre-distort the signal at the transmitter. The filter architecture consists of electrical components like an FPGA for memory requirements , D/A converter to re-construct the analog signal for precision, and digital signal processing (DSP) in the background to achieve pre-distortion in the electrical domain. Electrical domain pre-compensation has advantages over optical dispersion compensation in terms of cost, flexibility, tuning and reproducibility. The design of the processor architecture is illustrated in the Figure (5.1).

The input data is considered to be an infinite bit sequence consisting of 1's and 0's. In this paper, these bits are represented as NRZ pulses with equal rise time and time of 15% of bit period. To achieve the same bit sequence at the receiver, we need to pre-distort the input data using DSP and DAC.

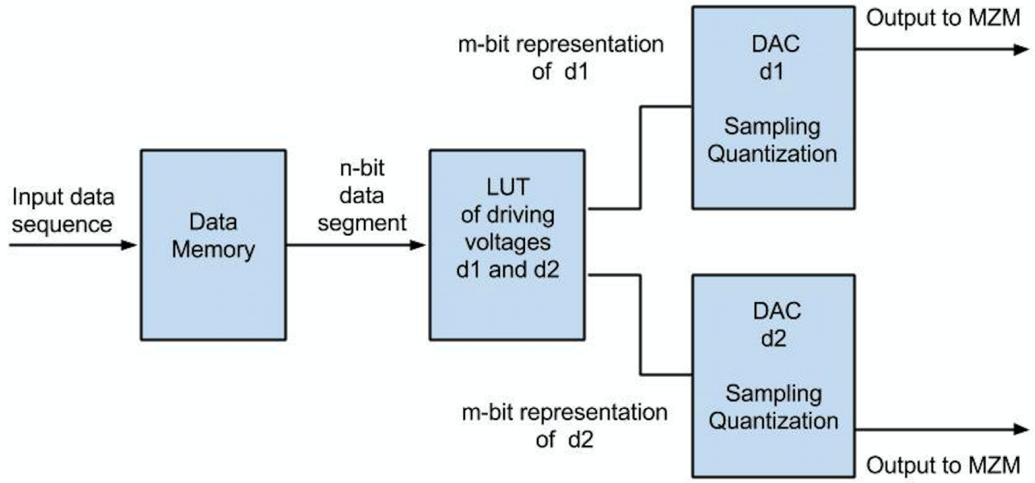

Figure 5.1: Digital processor architecture

5.2 Memory

The input bit sequence is stored in high speed static access memory that can be achieved by using a high end FPGA like Altera DE boards or Xilinx. For numerical analysis, we are using register or a variable to store each input sequence. The memory will release the stored data as a sequence of segments of n bits. Total number of output segments is given by $2^n - n + 1$. For example, consider an initial data sequence of '10110011' and segment of n =3 . The memory will release this sequence in 6 segments of 3 bits, and each segment will step by one bit as follows : 101, 011, 110, 100, 001, 011. Each of these data segments is sent to and processed by the look-up table (LUT).

5.3 Look-up Table

The RAM-based look-up table (LUT) is defined as a table of stored estimate values, which are used to compare the feedback received from the receiver and the transmitter and then correct the estimates to obtain precision. In this digital revolution, there is an increase in the processing capability and memory storage of RAM that serves a immediate purpose for research studies that involves heavy processing and iterations to obtain simulated data. Look-up table are used to increase the processing time to retrieve a value from memory rather than old school input/output operation which saves time and reduces computing process complexity[11].

To understand the design of LUT, for simplicity, we have used LUT as a collection of variables that stores the digital bits of driving voltages that corresponds to the construction of pre-distorted signal. Each segment of length n bits from the memory unit are sent as an input to the the look-up table (LUT) to perform the digital signal processing on each input segment and sample the driving voltages required to obtain the pre-distorted signal. Each processed output is then sampled to give a desired m bit word that determines the resolution of Digital-to-analog converter (DAC). This m bit word which represent the driving voltages are binary bits are sent to DAC for re-construction of driving voltages d1 and d2 to drive the dual-drive MZM to generate a pre-distorted signal. For example the bit pattern [0 1 1] will be mapped to a specific pre-distortion signal for d1 and d2.

The length of the LUT must accommodate all input segments and it is given by $2^n - n + 1$. The values stored in the LUT are obtained from the following equations Eq.(3.2), Eq.(3.8), Eq.(4.18) and Eq.(4.19):

$$tildeE_{dc}(0,\omega) = \tilde{E}(L,\omega)H^{-1}(\omega), \tag{5.1}$$

$$\tilde{E_{dc}}(0,T) = \sqrt{P_{dc}(0,T)}exp(i\phi(L,T)), \tag{5.2}$$

$$\nu_1 = \frac{1}{\pi S_1}\Big[\frac{\pi}{2} - \phi_{dc}(0,T) \mp \arcsin\Big(\sqrt{\frac{P_{dc}(0,T)}{P_{in}}}\Big)\Big] - \nu_{b1}, \tag{5.3}$$

and

$$\nu_2 = \frac{1}{\pi M S_2}\Big[\frac{\pi}{2} - \phi_{dc}(0,T) \pm \arcsin\Big(\sqrt{\frac{P_{dc}(0,T)}{P_{in}}}\Big)\Big] - \nu_{b2}. \tag{5.4}$$

Let $\tilde{E}(L,\omega)$ be the desired spectrum of the input bit sequence and $\tilde{E}(0,\omega)$ be the pre-distortion signal. Pre-distortion signal in the time-domain $\tilde{E_{dc}}(0,T)$ is obtained by doing inverse Fourier transform and is used in the Eq (5.3) and (5.4) to calculate the voltages required to drive the MZM. Thus we can say, for every consecutive n-bit input sequence, LUT gives digital bits that corresponds to analog voltages of d1(t) or d2(t) at the output. These LUT values can be varied by changing the dispersion length L_D, β_2, T_0.

5.4 Digital-to-Analog converter

Digital-to-Analog converter (DAC) is one of the integral electrical component that is used to study the analysis of signal in signal processing applications. By definition, it is used to convert binary bits into a analog signal, analog signal can be used to represent either current, voltage or any electrical parameter based on the application. Digital data is favored to analog form in the following ways:

- Ease of transmission: if data is too long, it can be divided into small chunks of data and can be transmitted and re-produced at the expense of complexity at the receiver.
- Secure communication: For security purposes, digital data can be easily encrypted and cyclic redundancy check ensures integrity of the data.
- Transmission speed: Digital data can be transmitted at a faster rate and can be made to take a shortest path to reach the destination at the expense of resolution of data.

It's counterpart analog-to-digital converter (ADC) has been used in vast applications, however, the usage of DAC in applications have been slightly increased lately in 2010, with the advent of lower power consumption electronics and increase in data-processing capabilities, more research is put into areas where the conversion from digital domain to analog domain is used to abstract critical data to asses the quality of the signal. Few research areas include voice over internet (VOIP), audio speakers,etc.

In general, DAC are used to convert sampled finite-precision time-series data into a continuous form of an analog signal. Typical operation of DAC includes converting abstract values into a sequence of impluses that are then processed by re-construction algorithm to fill the gap between the sampled data. Digital-to-analog conversion is characterized by the following factors:

- Resolution: Number of bits that is used to represent the sampled data in the form of an output levels is termed as resolution. number of output levels are

given in the form of 2^n, where n is the number of resolution. It ranges from 3 to 128 based on device capability. For example, if resolution is 3, number of output levels generated are $2^3 = 8$. Resolution can be increased to increase the accuracy of the output analog signal.

- Smapling rate: The rate at which DACs operate to maintain the accuracy of the output.

5.4.1 Analysis

To explain the functioning of a typical DAC, let us consider a sine wave written in the form

$$y = abs(10sin(t)), \tag{5.5}$$

where t is a time vector ranging from 0 to 10 in 100 points with an interval of 0.1 [ps]. If the resolution of DAC is considered to be 3, then quantization interval is given by

$$q = \frac{U}{(2^n - 1)}, \tag{5.6}$$

where U is the amplitude of the input signal, and n is the resolution of the DAC. Then signal is processed to obtain the digital bits which act as an input to the DAC which can be written as

$$\begin{aligned} a &= fix(y/q), \\ yd &= dec2bin(a, n), \end{aligned} \tag{5.7}$$

where a is the sampled input and dec2bin is the function in Matlab used to convert the decimal values to the binary bits based on the resolution of the DAC. Now,

multiplying the sampled input with the quantization interval gives re-constructed analog signal whose characteristics can be altered by the resolution and sampling algorithm. Re-constructed signal is shown in the Figure (5.2) and is given by

$$yq = a * q. \tag{5.8}$$

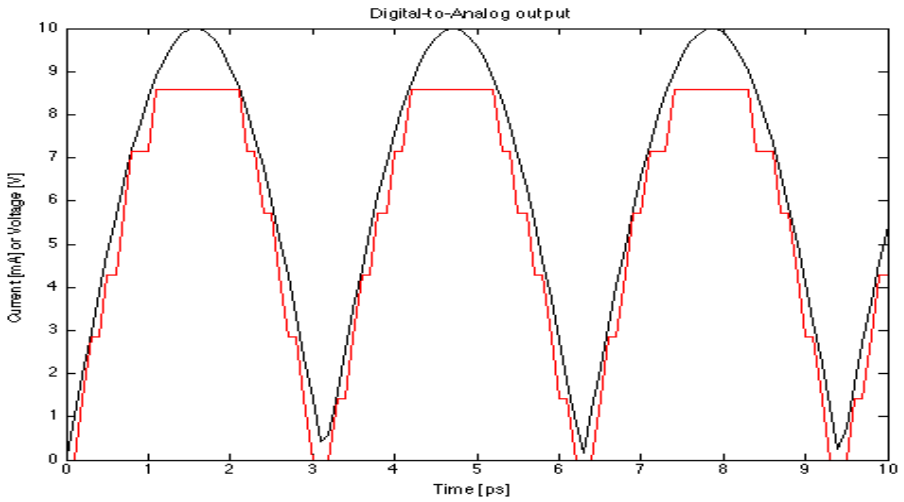

Figure 5.2: Operation of a DAC with $resolution = 3$

Driving voltages d1 and d2 obtained from LUT are represented in binary levels using m bits for each symbol period. Each memory segment is converted to two m-length word, one for d1 and one for d2. Accuracy and precision of the analog voltages can be increased by varying the sampling rate and vertical resolution, given by 2^m. The sampling rate is given by $S = C_s R_s$, where R_s is the baudrate and C_s is a scaling factor.

Consider the analog drive signals d1 and d2 shown in the Figure (5.3). The points are created at an interval of T_s. The point at t_1 for each signal , for example, comes from a single m-length word stored in the LUT. Each of the two words is related to the same n-bit segment.

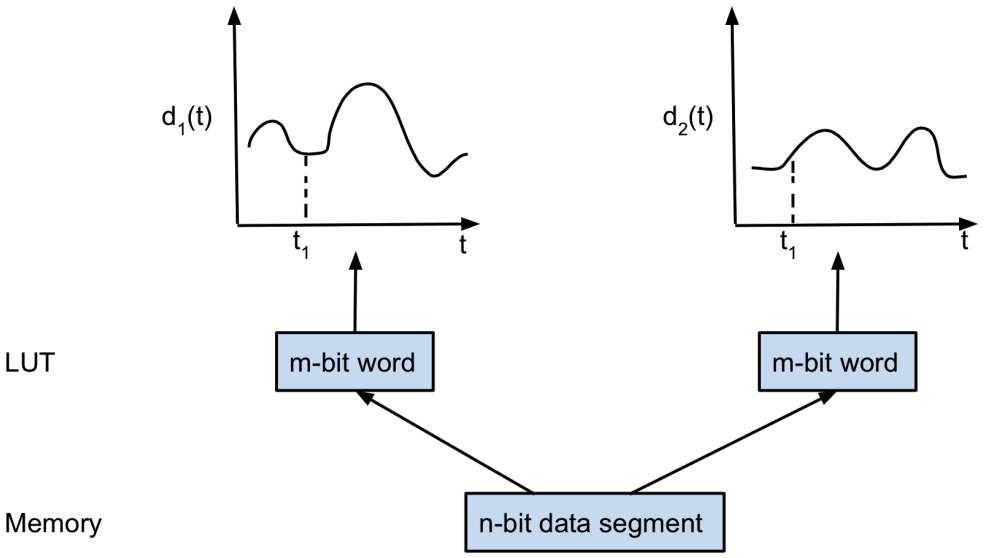

Figure 5.3: Digital-to-analog converter

Now, the performance of the system can be assessed by the parameters like n-bit length, length of the fiber, sampling rate and quantization bits of the D/A converter.

Chapter 6

Pre-distortion Model

The focus of my thesis is to investigate and re-produce the characteristics implemented in a electronic dispersion pre-compensation (EDP) technique using a Dual-drive Mach-Zehnder modulator(MZM) at the transmitter depicted in Figure (6.1).

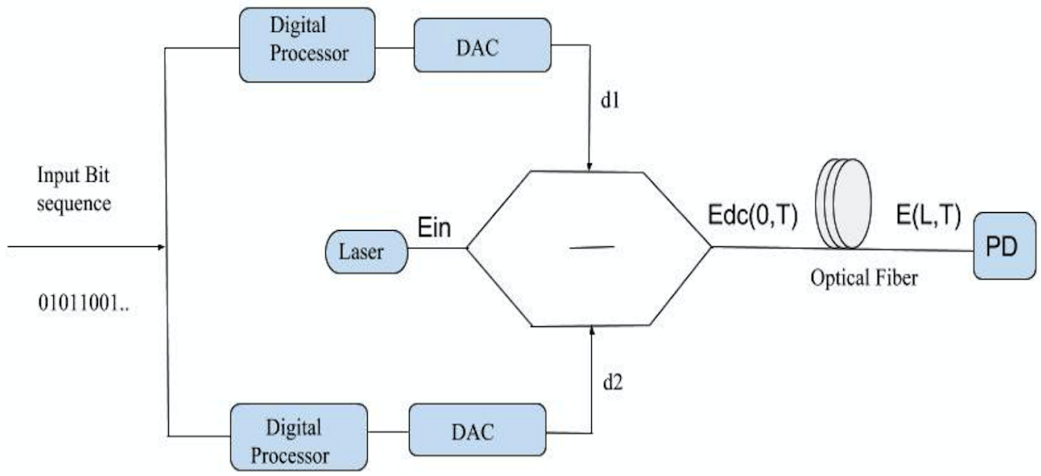

Figure 6.1: Model design to achieve pre-distortion

As discussed earlier in chapter 3, pre-distortion model is implemented to counter the linear transmission impairments produced during the signal propagation in an optical fiber. The technique is to pre-distort the signal at the transmitter in the electrical domain to deliver the desired optical signal at the receiver. Electrical domain is chosen as opposed to optical domain due to it's computational process in both offline and realtime and in an effective, economical and fast way.

As shown in the Figure (6.1), electrical components such as memory unit, digital signal processor , and digital and analog converter are used to process the signal at the transmitter, where optical components such as dual-drive MZM, laser source, optical fiber and photo-detector are used to derive the optical signal needed for analysis in both optical domain and electrical domain.

6.1 Analysis

Let us discuss the steps to analyze the pre-distortion using a single gaussian pulse.

1. **Define** $P_{des}(L,T)$

Using Eq.(3.2), let $P_{des}(L,T)$ be the desired received power and $E_{des}(L,T)$ be the desired optical signal at the receiver which can be written in the form

$$E_{des}(L,T) = \sqrt{P_{des}(L,T)}exp(i\phi_{des}(L,T)). \tag{6.1}$$

The photo-diode at the receiver will measure $P_{des}(L,T)$, but $\phi_{des}(L,T)$ also exists. A dual-drive MZM is used to generate the desired signal with an amplitude and phase as discussed above . Let ds1 and ds2 be the voltages normalized to $V\pi_1$ driving the MZM take the shape of a simple gaussian pulse as shown in the Figure (6.2), but opposite in sign given by

$$\begin{aligned} ds1 &= A_0 \exp(-\frac{T^2}{2T_0^2}), \\ ds2 &= -A_0 \exp(-\frac{T^2}{2T_0^2}). \end{aligned} \tag{6.2}$$

where A_0 is the initial amplitude of the signal.

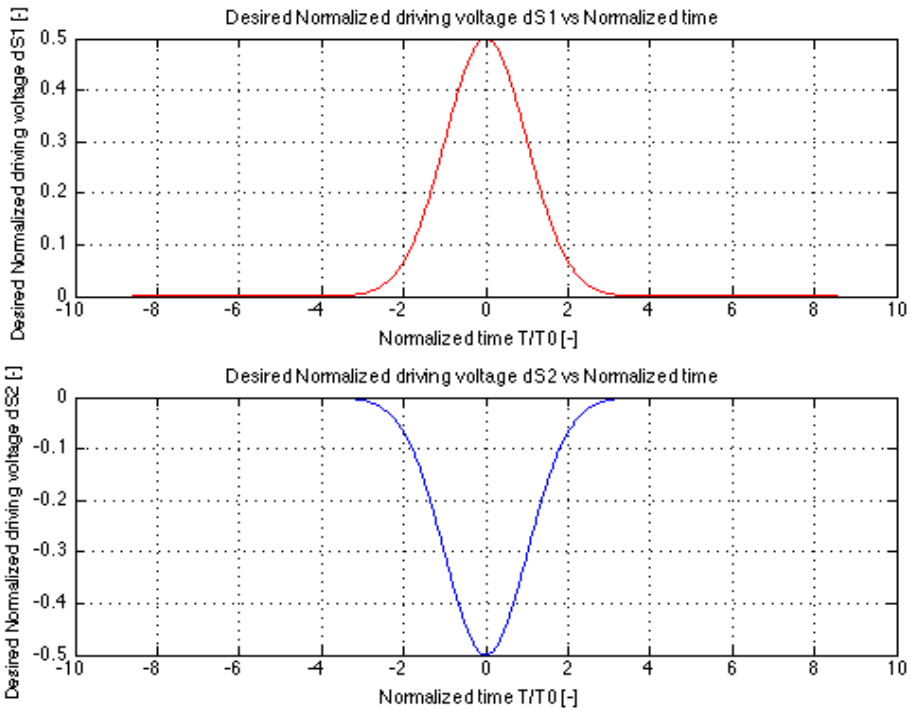

Figure 6.2: Driving voltages ds_1 and ds_2 to obtain desired optical signal $E_{des}(L,T)$

Using Eq. (4.1), (4.6) and (4.7), desired optical signal at the receiver $E_{des}(L,T)$ is obtained as shown in the Figure (6.3) and is given by

$$E_{des}(L,T) = Ein \sin(\phi_1) \exp(i\phi_2), \tag{6.3}$$

where E_{in} the input signal generated by a continuous wave laser source and is used as a constant value in the analysis.

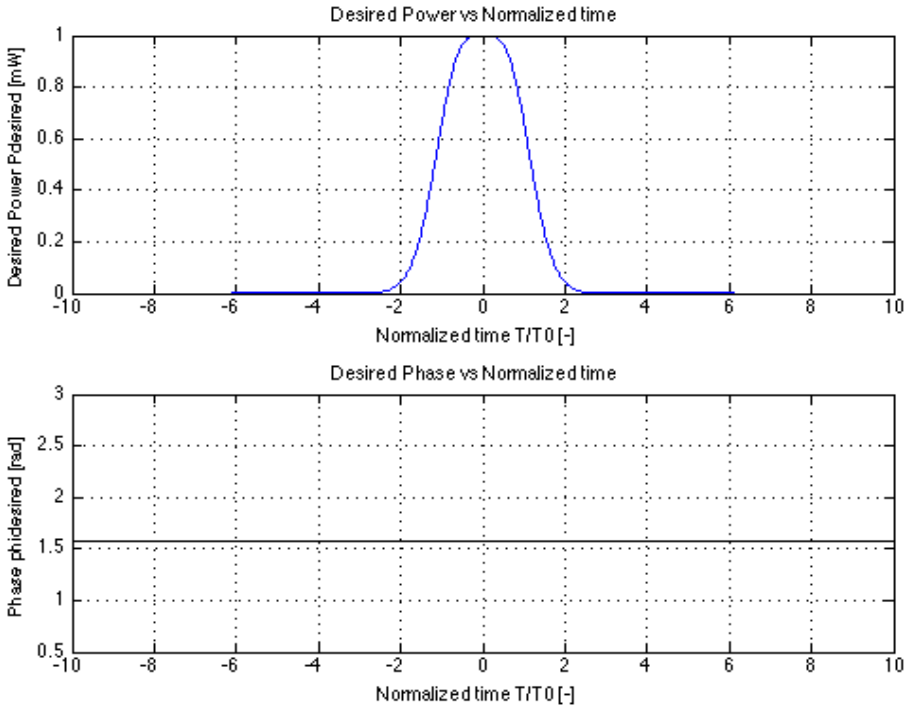

Figure 6.3: Desired power and phase of an optical signal $E_{des}(L,T)$

Phase components ϕ_1 and ϕ_2 can be written as

$$\phi_1 = (-\frac{\pi}{2})S_1(ds_1 + V_{b1}) - (-\frac{\pi}{2}))MS_2(ds_2 + V_{b2}), \tag{6.4}$$

and

$$\phi_2 = (-\frac{\pi}{2})S_1(ds_1 + V_{b1}) + (-\frac{\pi}{2}))MS_2(ds_2 + V_{b2}) + \frac{\pi}{2}. \tag{6.5}$$

where S_1 is the sign of electro-optic parameter μ_1 and S_2 is the sign of μ_2 that are sought to be equal and absolute value of $\frac{\mu_2}{\mu_1}$ given by M is considered as a constant value 1.

2. **Calculate** $E_{des}(L,\omega)$

Using FFT function in Matlab, Electric field of a desired optical signal at the receiver in frequency domain is shown in the Figure (6.4).

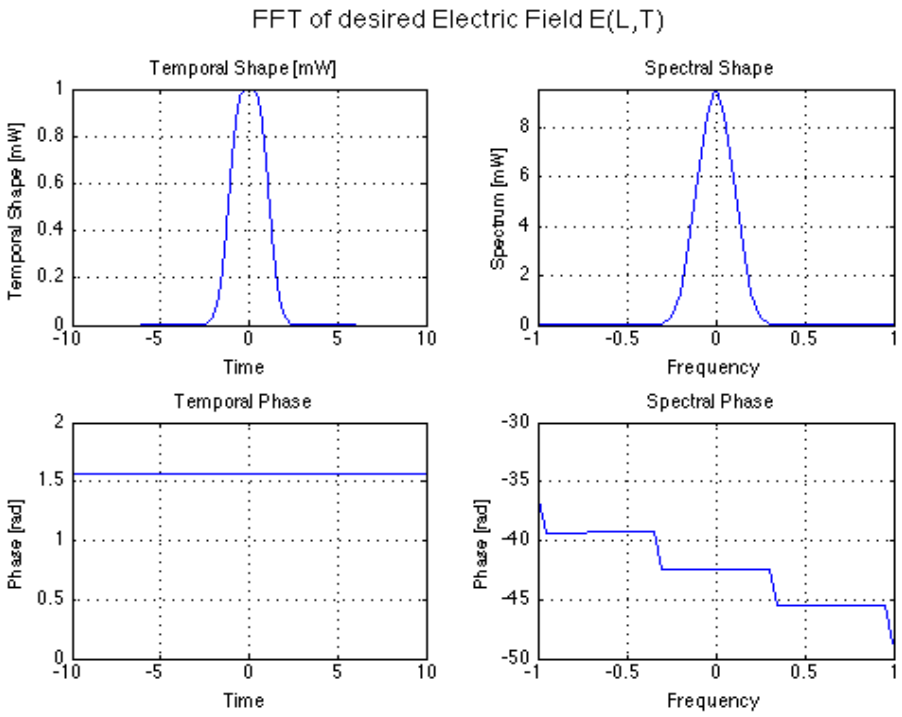

Figure 6.4: Power and phase of a desired optical signal $E_{des}(L,\omega)$

3. **Calculate** $E_{dc}(0,\omega)$ **using** $H(\omega)$

Using transfer function in Eq. (2.16), desired optical signal at the receiver is processed using DSP to produce the pre-distorted signal $E_{dc}(0,\omega)$ in the frequency domain is given by

$$E_{dc}(0,\omega) = E_{des}(L,\omega)H^{-1}(\omega). \tag{6.6}$$

where $H(\omega)$ is the transfer function. Using Eq. (2.41), Eq.(6.6) can be written as

$$E_{dc}(0,\omega) = E_{des}(L,\omega)\exp(-\frac{i}{2}sgn(\beta_2)(2\pi f)^2\frac{z}{L_D}). \tag{6.7}$$

where $\omega = 2\pi f$, $sgn(\beta 2)$ is the sign of a GVD parameter and $\frac{z}{L_D}$ is the normalized length of an optical fiber.

4. **Calculate** $E_{dc}(0,T)$

Using IFFT function in Matlab, calculate the pre-distorted signal in time domain, $E_{dc}(0,T)$. The pre-distorted signal in time domain for each value of normalized length is shown in the Figures below.

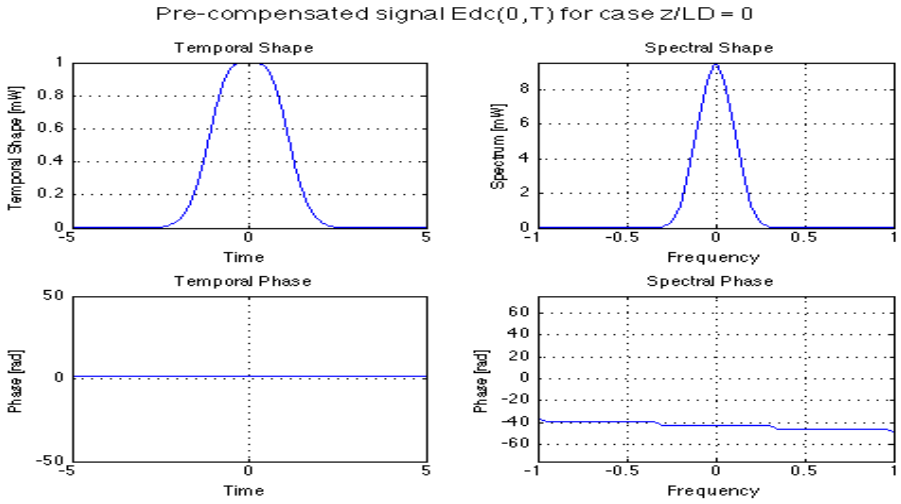

Figure 6.5: Power and phase of a pre-distorted signal $E_{dc}(0,T)$ at $\frac{z}{L_D} = 0$

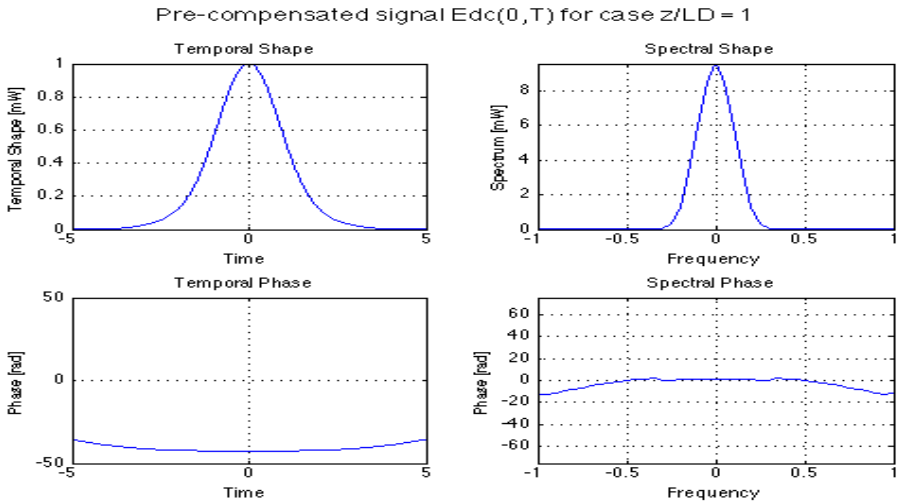

Figure 6.6: Power and phase of a pre-distorted signal $E_{dc}(0,T)$ at $\frac{z}{L_D} = 1$

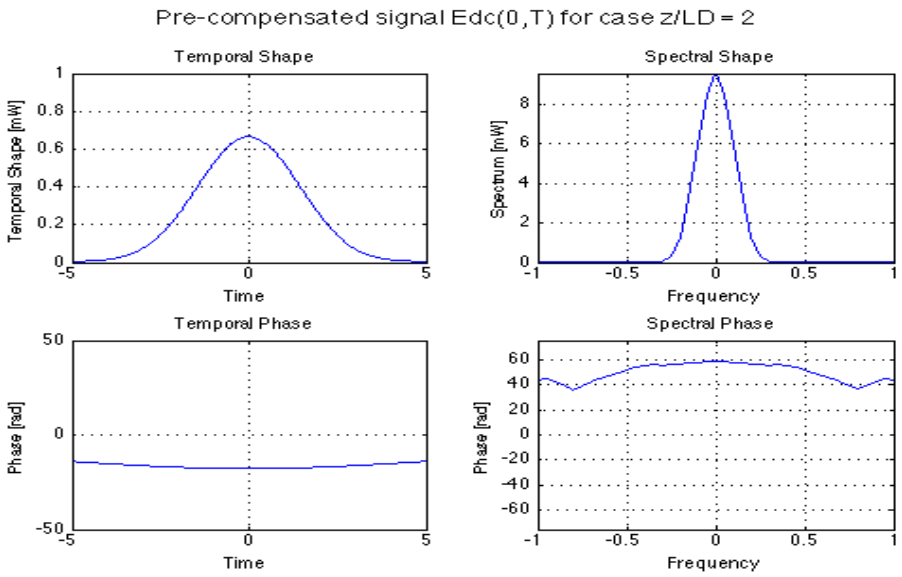

Figure 6.7: Power and phase of a pre-distorted signal $E_{dc}(0,T)$ at $\frac{z}{L_D} = 2$

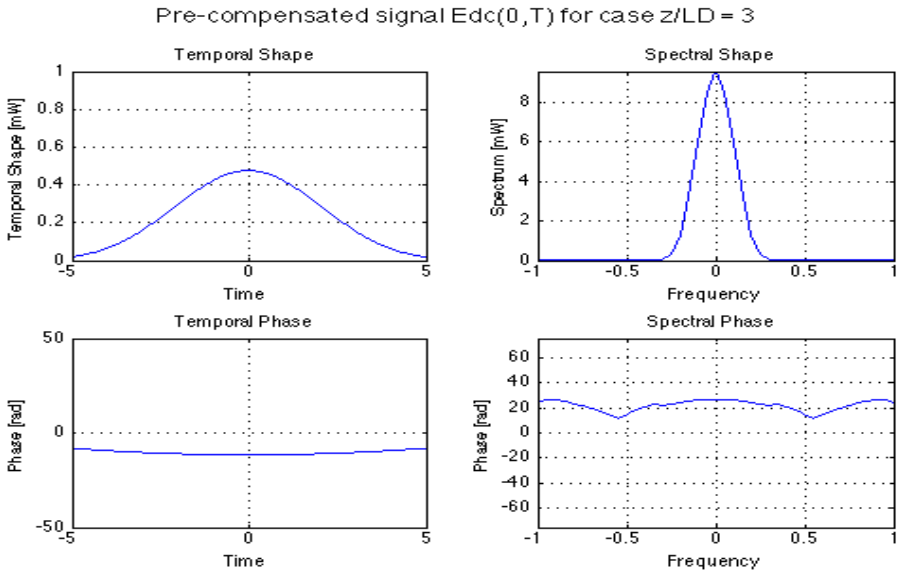

Figure 6.8: Power and phase of a pre-distorted signal $E_{dc}(0,T)$ at $\frac{z}{L_D} = 3$

5. **Calculate driving voltages $d_1(t)$ and $d_2(t)$**

Using Eq.(3.14), (4.18) and Eq.(4.19), derive the driving voltages $d_1(t)$ and $d_2(t)$ normalized to $V\pi_1$ that are required to generate a pre-distorted signal. This gives an in-depth analysis of how a dual-drive MZM is driven, biasing conditions and voltage swings of a RF signal. The normalized driving voltages $d_1(t)$ and $d_2(t)$ for each value of normalized length are shown in the Figure (6.9).

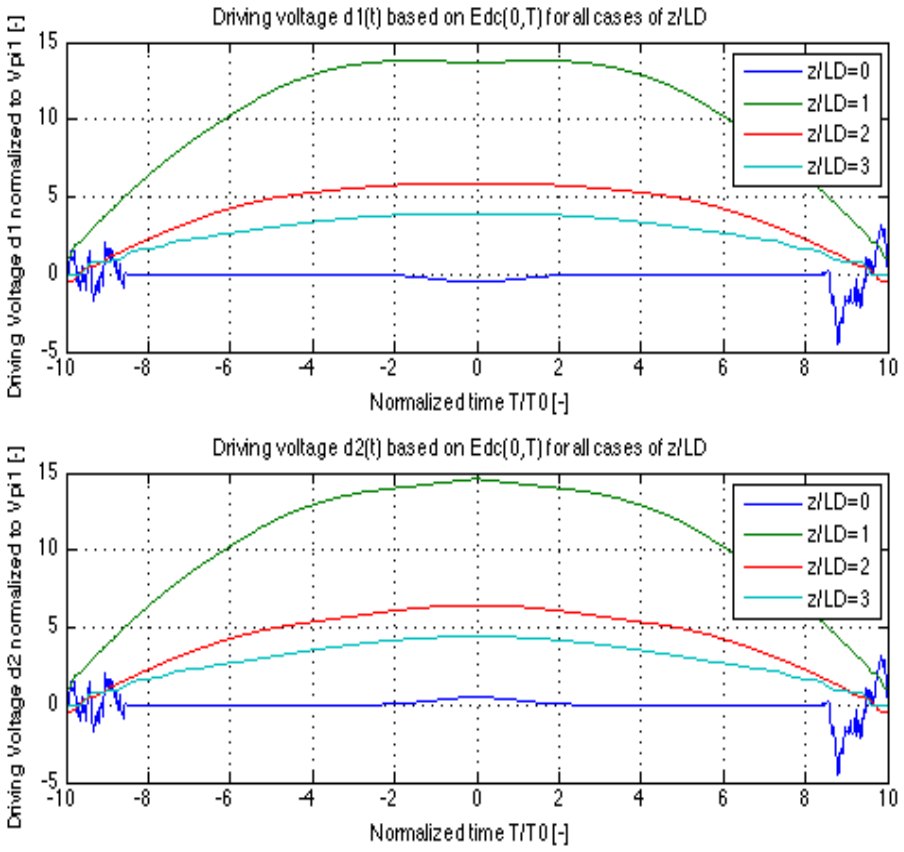

Figure 6.9: Driving voltages $d_1(t)$ and $d_2(t)$ for all cases of $\frac{z}{L_D}$

6. **Calculate** $E(L, \omega)$

Now when a pre-distorted signal is allowed to propagate in an optical fiber, pre-distortion reverse the linear impairment of dispersion in an optical fiber giving the desired the optical signal at it's output. Using Eq. (6.7), Electric field of a optical signal at the output of an optical fiber in the frequency domain, $E(L, \omega)$ is given by

$$E(L, \omega) = E_{dc}(0, \omega) \exp(\frac{i}{2} sgn(\beta_2)(2\pi f)^2 \frac{z}{L_D}). \tag{6.8}$$

7. **Calculate** $E(L, T)$

Using IFFT function in Matlab, calculate the received optical signal in time domain, $E(L, T)$. Received optical signal at the end of an optical fiber in time domain for each value of normalized length are shown in the Figures below.

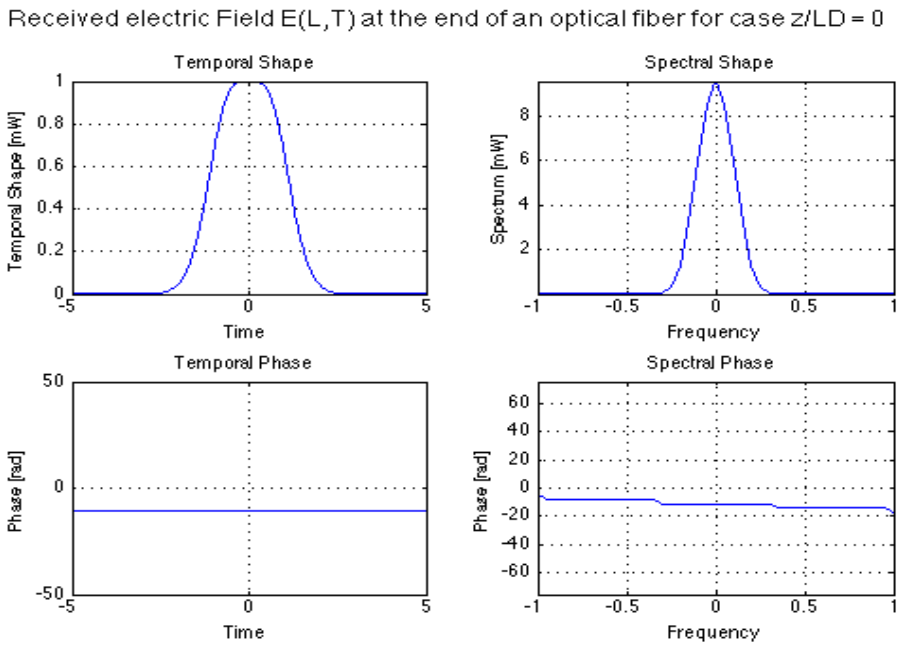

Figure 6.10: Power and phase of a received signal $E(L, T)$ at $\frac{z}{L_D} = 0$

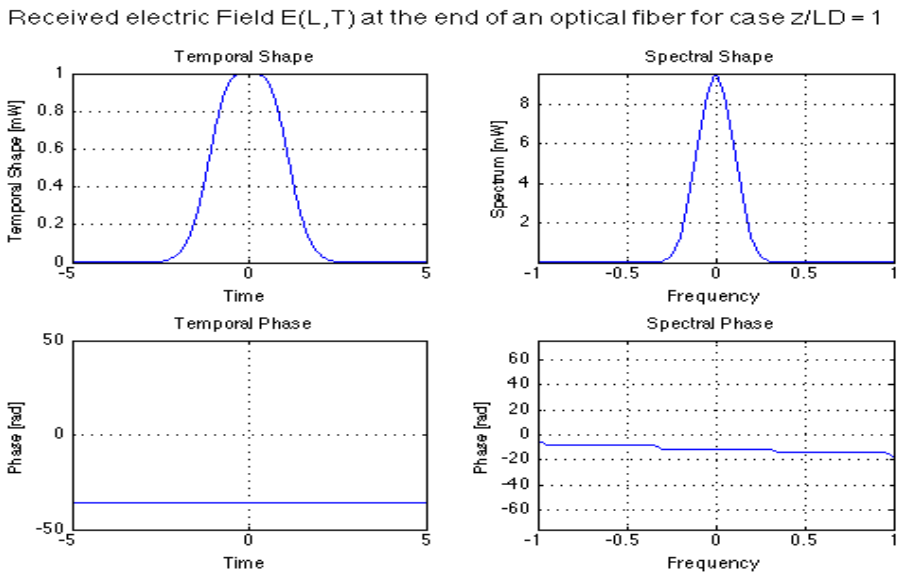

Figure 6.11: Power and phase of a received signal $E(L,T)$ at $\frac{z}{L_D} = 1$

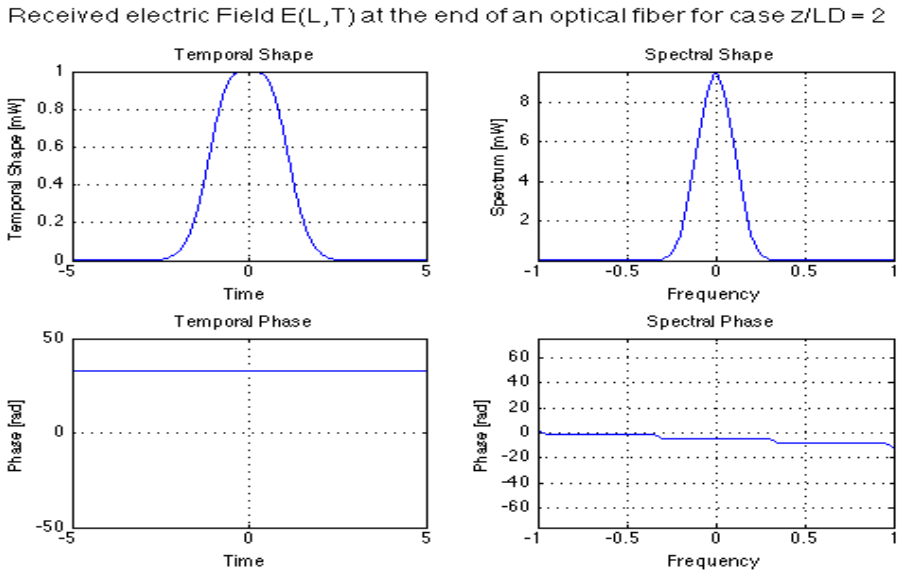

Figure 6.12: Power and phase of a received signal $E(L,T)$ at $\frac{z}{L_D} = 2$

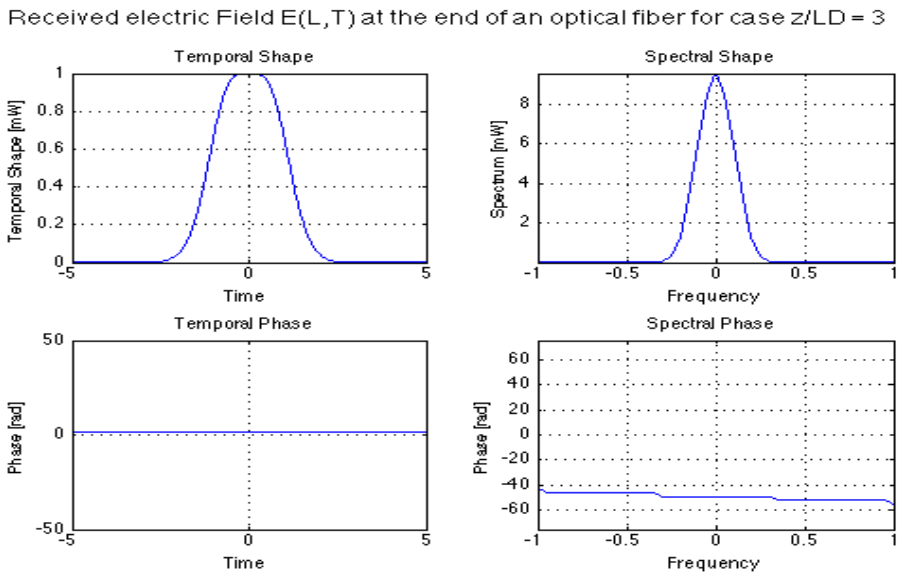

Figure 6.13: Power and phase of a received signal $E(L,T)$ at $\frac{z}{L_D} = 3$

8. **Sanity check**

As a sanity check, desired signal and received signal are compared to illustrate the accuracy of this model and undergo investigation against various parameters involved in the analysis. Plot for differences of desired signal $P_{des}(L,T)$ and received optical signal at the output of an optical fiber $P(L,T)$ for different values of normalized length is shown in the Figure (6.14).

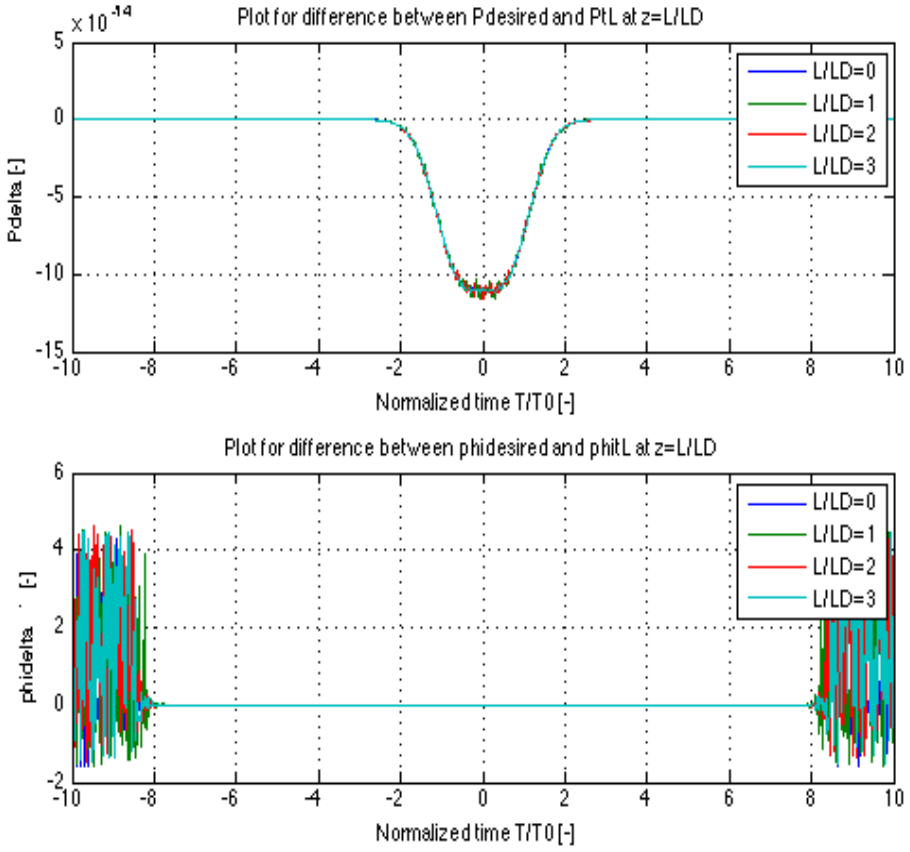

Figure 6.14: Difference between the desired and the received optical signal

Chapter 7

Eye-diagram analysis for a NRZ pulse

In the previous chapter, we have analyzed the process of pre-compensation technique using a gaussian pulse, however, to investigate in-depth in industry standards, a NRZ pulse is used as an input signal. A NRZ pulse gives a good understanding of dependent nature of pre-distortion technique on various parameters that are measured in terms of an eye penalty. In the pre-distortion model shown in the Figure (6.1), a input sequence of 1's and 0's are used as an input signal to the digital processor for signal processing. Let us discuss the steps involved in study of pre-distortion using a NRZ pulse.

1. **Input Sequence**

A Pseudo random bit sequence (PRBS) generator is used to create a PRBS sequence of 1's and 0's of order n. The length of the sequence is given by 2^n, where n is the order ranging from 1 to 32 or higher. This input sequence is given as an input to the digital signal processor for processing the signal to generate a pre-distorted signal. The input sequence is windowed into n-bit segment for which study of effect of pre-distortion is analyzed on the center bit of the each individual n-bit segment. The number of n-bit segments is given by $2^n - n + 1$. Let us consider a PRBS sequence of order 3, then length of the sequence given by 2^n is 8 and number of individual segments given by $2^n - n + 1$ is 6.

2. **Desired optical signal** $P_{des}(L,T)$

Let us consider driving voltages $ds_1(t)$ and $ds_2(t)$ normalized to $V\pi_1$ take the shape of a NRZ pulse encoding the PRBS sequence of order 3. Upon biasing the dual-drive MZM at the biasing point of 1.25 [-] and RF voltage swing of: -.25 and +0.25, desired signal $P_{des}(L,T)$ is obtained. Using pattern generator object in Matlab, a NRZ pulse is constructed for each 3-bit segment with a combined rise time and fall time of 30 [ps] as shown in the Figure (7.1).

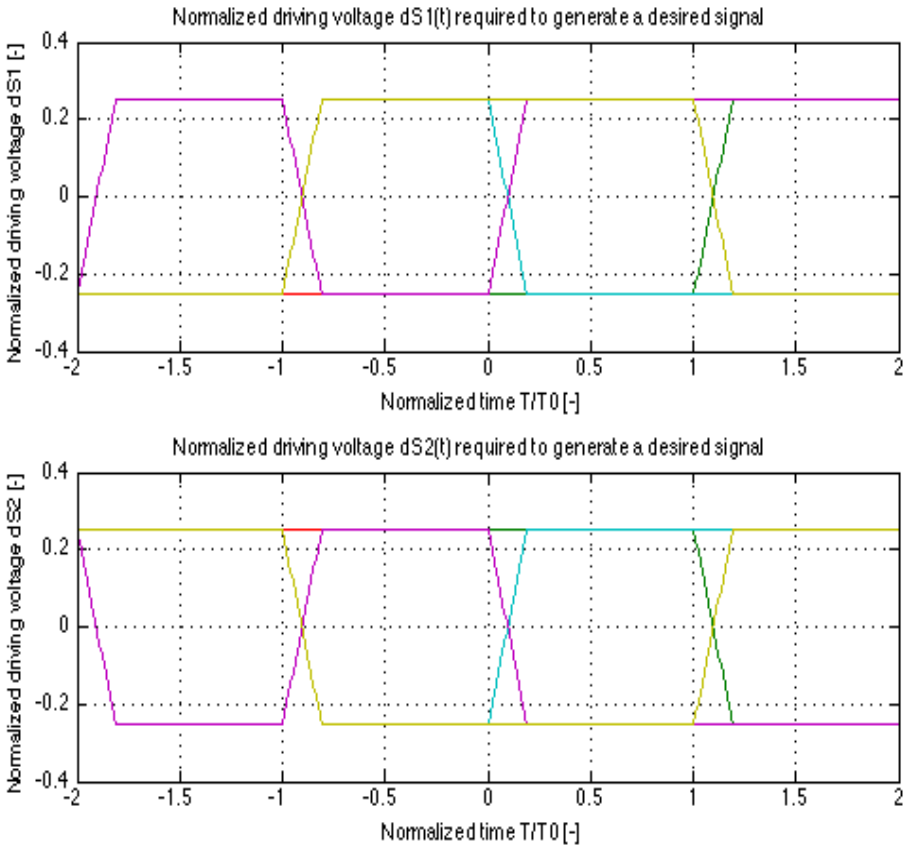

Figure 7.1: Normalized driving voltages $ds_1(t)$ and $ds_2(t)$ required to construct $P_{des}(L,T)$

The desired optical signal $P_{des}(0,T)$ at the receiver constructed using a dual-drive MZM is shown in the Figure (7.2).

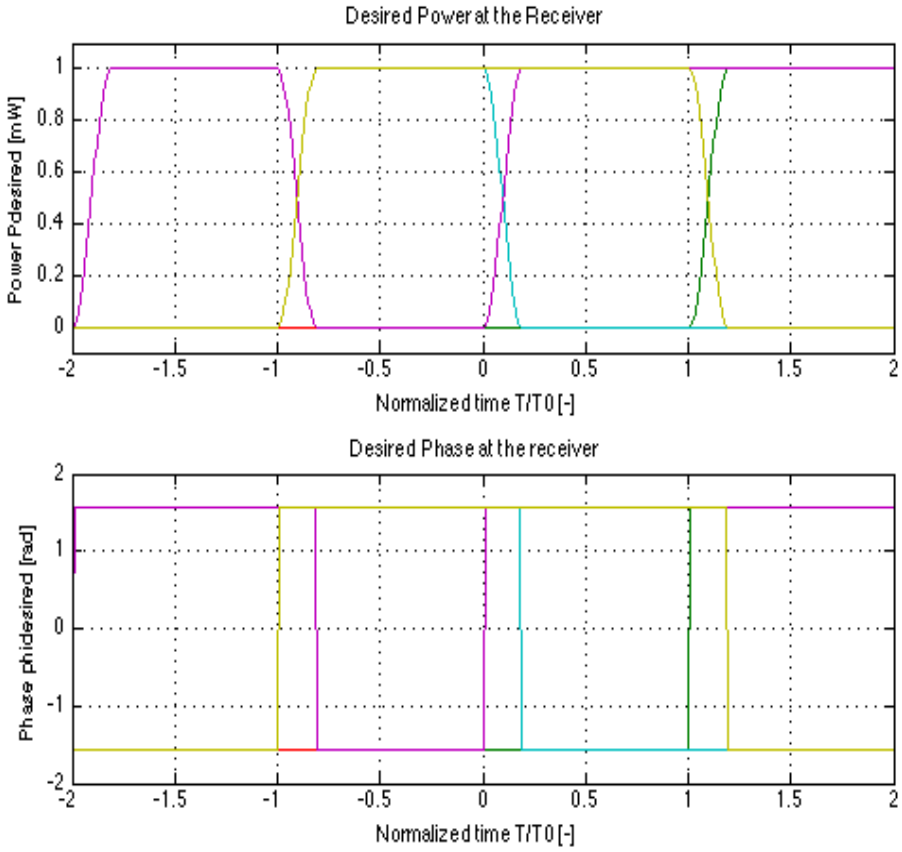

Figure 7.2: Desired optical signal at the receiver $P_{des}(L, T)$

3. **Calculate driving voltages $d_1(t)$ and $d_2(t)$**

Using Eq.(3.14), (4.18) and Eq.(4.19), driving voltages $d_1(t)$ and $d_2(t)$ normalized to $V\pi_1$ that are required to generate a pre-distorted signal are calculated. Once obtained, values of driving voltages are stored in the look-up table register to sample the input signal and convert to binary bits for re-construction of signal using a DAC. For a normalized length $\frac{z}{L_D}$ value of 2, normalized driving voltages $d_1(t)$ and $d_2(t)$ for all the input 3-bit segment are shown in the Figure (7.3).

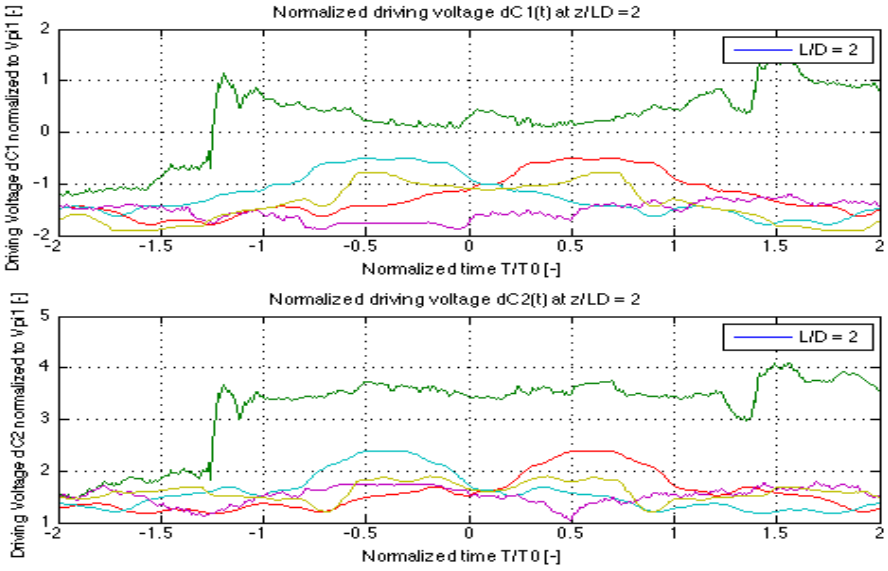

Figure 7.3: Normalized driving voltages $d_1(t)$ and $d_2(t)$ at $\frac{z}{L_D} = 2$

Let us consider the resolution of the DAC is 4, then re-constructed signal for all the input 3-bit segment at the output of the DAC is shown in the Figure (7.4).

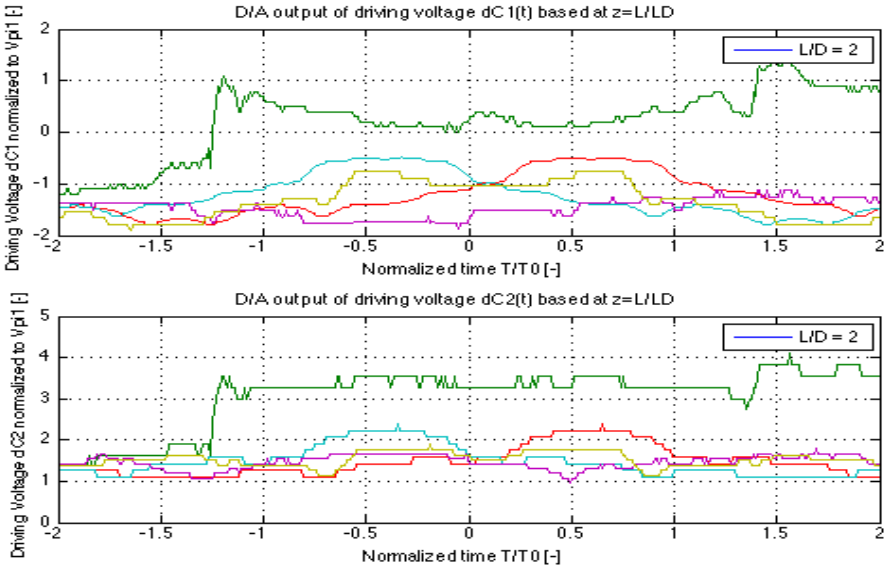

Figure 7.4: Re-constructed $\frac{D}{A}$ output of normalized driving voltages $d_1(t)$ and $d_2(t)$ at $\frac{z}{L_D}$ and $resolution = 4$

4. **Derive pre-distorted signal** $P_{dc}(0,T)$

The re-constructed driving voltages $d_1(t)$ and $d_2(t)$ are used to drive dual-drive MZM to construct a pre-distorted signal $P_{dc}(0,T)$ as shown in the Figure (7.5).

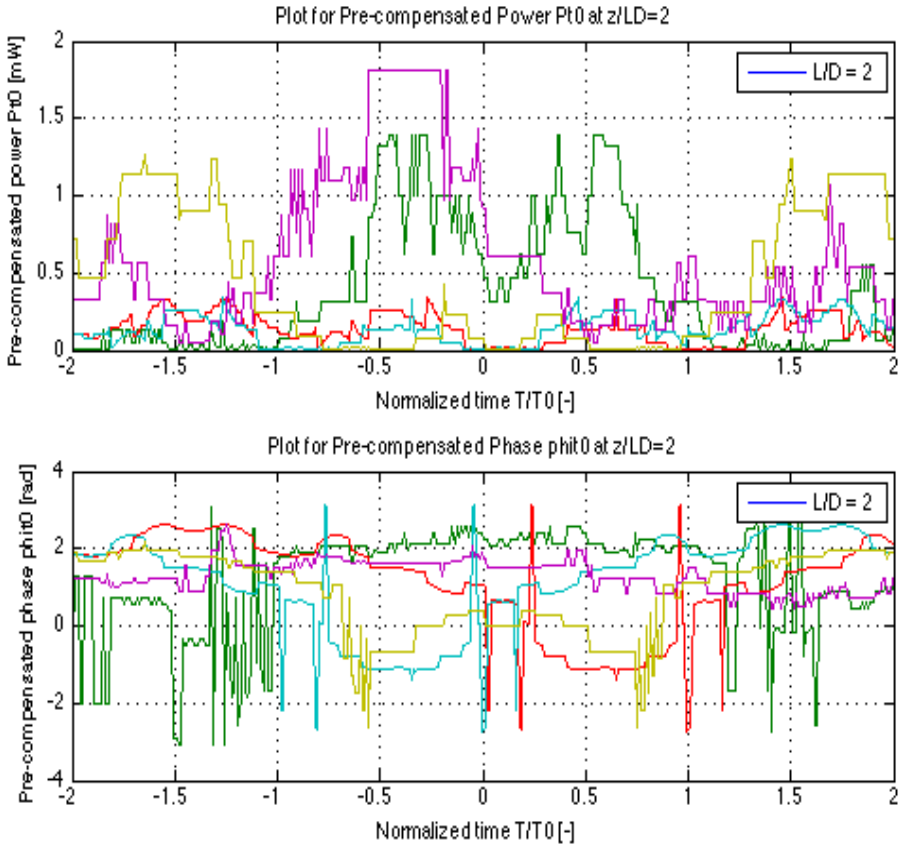

Figure 7.5: Pre-distorted signal $P_{dc}(0,T)$ at $\frac{z}{L_D} = 2$ and $resolution = 4$

5. **Calculate received optical signal at the end of an optical fiber** $P(L,T)$

When a pre-distorted signal is sent through an optical fiber, it reverses the chromatic dispersion in the linear medium of an optical fiber and generates a desired signal $P(L,T)$ at the end of an optical fiber as shown in the Figure (7.6).

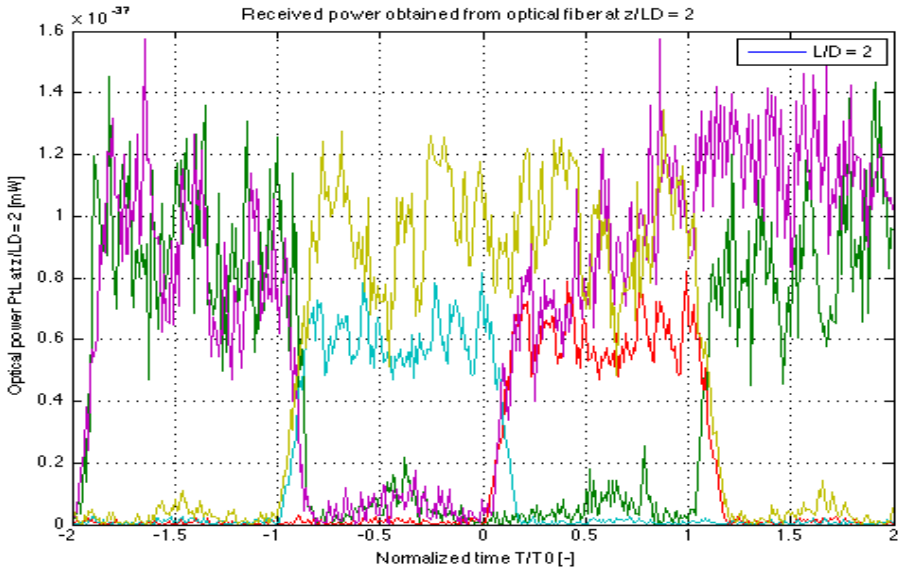

Figure 7.6: Received signal $P_{dc}(0,T)$ from an optical fiber at $\frac{z}{L_D} = 2$ and $resolution = 4$

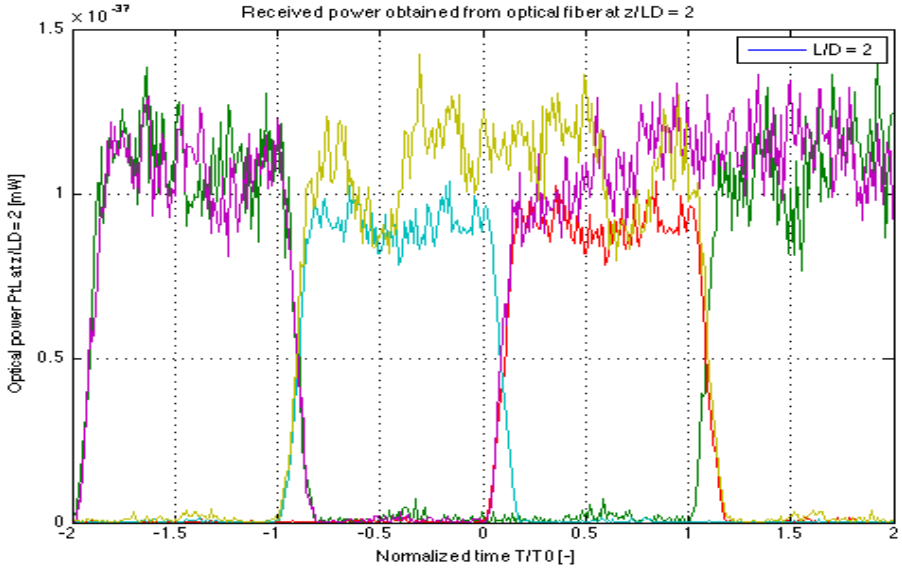

Figure 7.7: Received signal $P_{dc}(0,T)$ from an optical fiber at $\frac{z}{L_D} = 2$ and $resolution = 5$

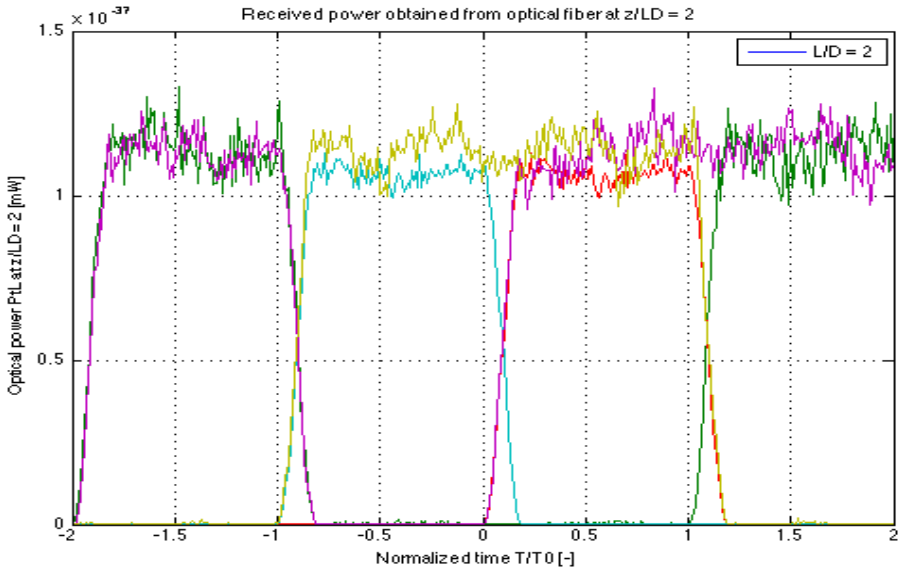

Figure 7.8: Received signal $P_{dc}(0,T)$ from an optical fiber at $\frac{z}{L_D} = 2$ and $resolution = 6$

From the Figure (7.6), (7.7) and (7.8), we can observe that increase in the resolution of the DAC, received signal at the output of an optical fiber looks less cluttering and gives a scope to understand the analysis of eye-opening for the center-bit for each n-bit sequence.

7.1 Eye-diagram analysis

To study the eye-diagram analysis, center bit of each n-bit sequence is considered due to effect of chromatic dispersion of adjacent bits in a sequence. Let us discuss the steps to calculate the eye-opening for the center bit of each sequence.

1. **Indices**

If t(n,m) is the time vector where n and m are indices of initial time and final time for the center bit, corresponding P(n,m) is calculated for each n-bit sequence to analyze the eye-opening for the center bit. Let us consider Figure (7.8) as an example to calculate the eye-opening. We can take time vector from -0.5 to -0.25 for the center bit that corresponds to indices 150 and 175 assuming 100 points per symbol. Now calculate the power (Y-axis) vector that corresponds to time vector,

i.e P(150,175) that results in either a column or a row vector.

2. **Windowing**

To create a upper eye window and a lower eye window, a threshold point is set which serves as a line that separates the eye into upper and lower window. Generally, threshold point can be written as

$$Threshold - pt = \frac{max(S) + min(S)}{2}. \tag{7.1}$$

where S in the input signal. Once threshold point is set, power plot corresponding to upper window $P(P > Threshold{-}pt)$ and lower window $P(P < Threshold{-}pt)$ are calculated for each m-bit segment.

3. **Concatenation**

Once power plot corresponding to upper and lower window for each 3-bit segment is calculated, then window parameters for all m-bit segments of n-bit sequence are obtained by the concatenation of P vector. Let us consider a null vector V_0 given by [ ]. Then Upper window vector V is given by

$$\begin{aligned} V &= V_0, \\ a &= P(P > Threshold), \\ V &= [V, a]. \end{aligned} \tag{7.2}$$

and Lower window vector L is given by

$$\begin{aligned} L &= V_0, \\ b &= P(P < Threshold), \\ L &= [L, b]. \end{aligned} \tag{7.3}$$

4. **Eye-opening**

After the calculation of concatenated vectors L and V for the upper and lower window, eye-opening in [dB] is given by

$$Eye_{opening} = 10log_{10}\big(mean(V) - 3 * std(V)) - (mean(L) + 3 * std(L)\big). \quad (7.4)$$

5. **Eye-penalty**

When a highest resolution of the DAC and normalized length $\frac{z}{L_D} = 0$ is taken, eye-opening for the back2back case is considered as a reference value. For example, for a PRBS sequence of order 3, and resolution of DAC equal to 7, eye-opening value is found out to be -0.0474 [dB]. Then Eye-penalty is defined as difference of eye-opening value for each n-bit sequence and the reference value which can be written in the form

$$Eye_{penalty} = Eye_{opening}seq - Eye_{opening}ref. \quad (7.5)$$

Now let us asses the performance of pre-distortion technique by measuring the eye-penalty against the parameters such as PRBS order of input sequence, resolution of DAC, and normalized length of the fiber $\frac{z}{L_D}$.

7.2 Eye-penalty vs Resolution of DAC

The plots of Eye-penalty against the resolution of digital-to-analog converter are shown in the Figure (7.9) and Figure (7.10). From the observations, we can conclude that as resolution of DAC increases, eye-penalty for different values of normalized length $\frac{z}{L_D}$ has been decreased and with respect to normalized length, EOP decreases with increase in value of $\frac{z}{L_D}$. Thus, resolution of DAC plays an important measure in calculating the eye-penalty and fidelity of the signal.

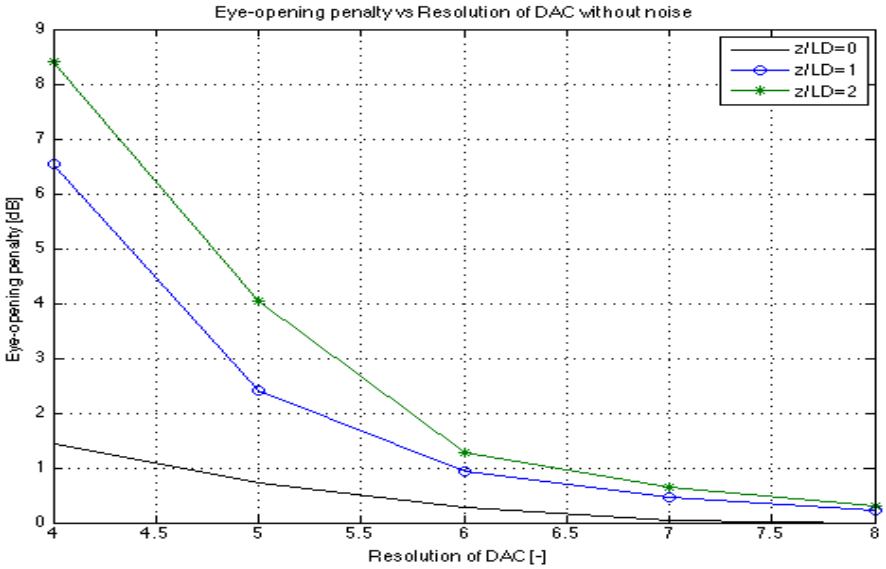

Figure 7.9: Eye-penalty vs Resolution of DAC for different values of normalized length $\frac{z}{L_D}$ without noise

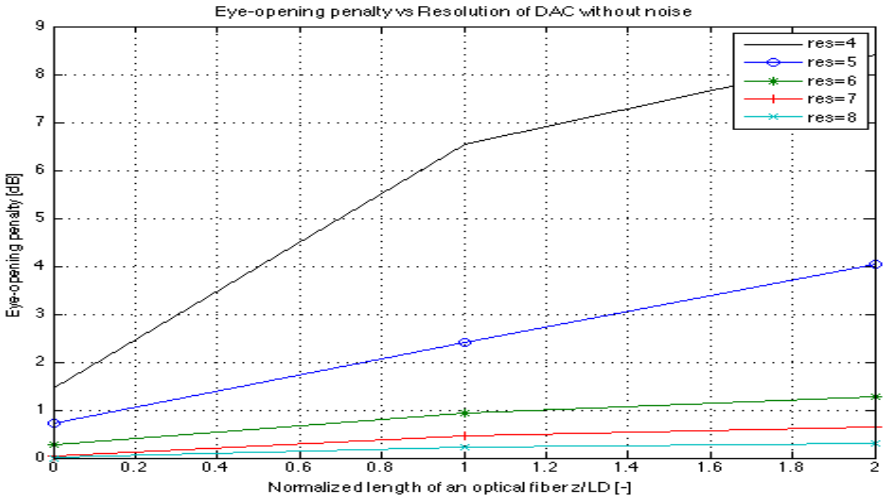

Figure 7.10: Eye-penalty vs Resolution of DAC for different values of normalized length $\frac{z}{L_D}$ without noise

7.3 Eye-penalty vs Order of PRBS sequence

The plot of Eye-penalty against the order of PRBS sequence employed as an input signal is shown in the Figure (7.11). From the observations, we can conclude that as the order of the sequence increases, computational process of the technique increases as well as decrease in the eye-penalty compared to each value normalized length $\frac{z}{L_D}$ for fixed value of resolution of DAC. Thus, we can say, as we input more sequences of higher order, there is a chance of increasing the fidelity of the signal with the downside of heavy computational processing.

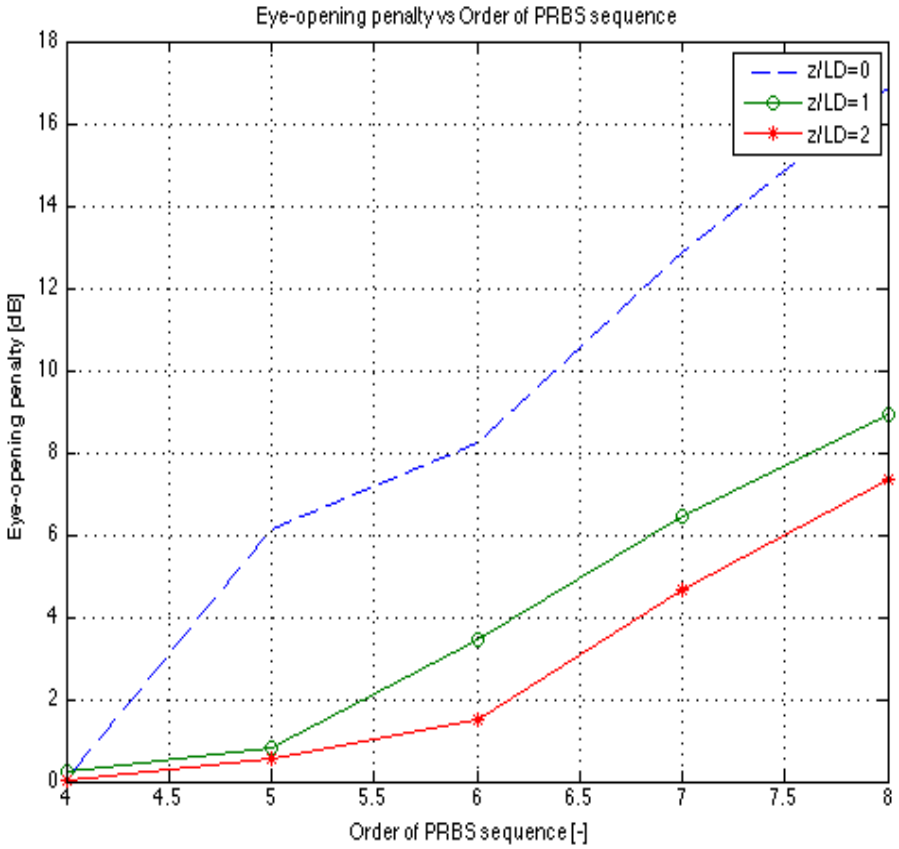

Figure 7.11: Eye-penalty vs Order of an input PRBS sequence for different values of normalized length $\frac{z}{L_D}$ and constant resolution of DAC

7.4 Noise analysis

In optical systems, there is noise present at the transmitter and receiver. In my thesis, we study different types of noise that are present and measure the signal characteristics against the electrical parameters discussed above. There are three types of noise, such as thermal noise, shot noise and relative intensity noise(RIN) each having it's own effect on the output signal received at the photodiode in this pre-distortion model.

7.4.1 Thermal noise

Thermal noise in general, affects the pulse at the zero level, so signal is bound to have noise at it's minimum level. In this investigation, we found effect of thermal noise follow the similar pattern with respect to the plot with a lateral shift in the EOP of a signal without noise for each value of normalized length as shown in the Figure (7.12).

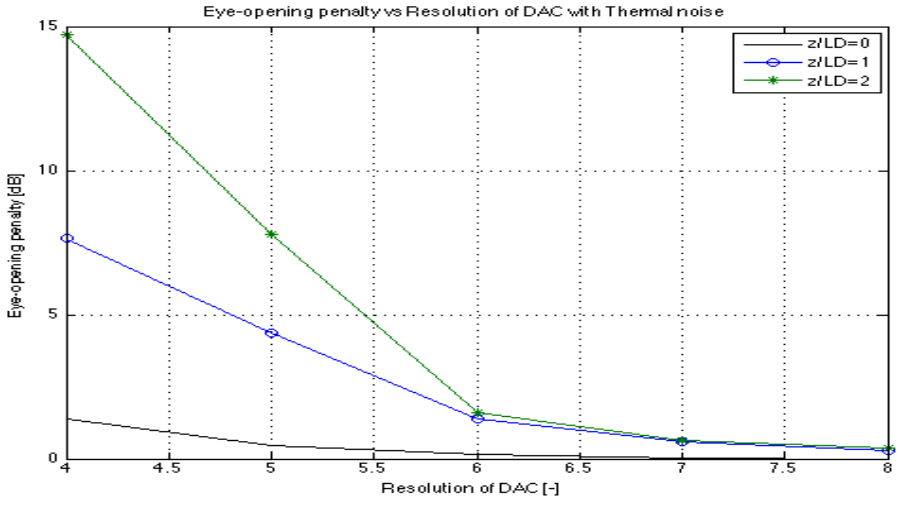

Figure 7.12: Eye-penalty vs Resolution of DAC for different values of normalized length $\frac{z}{L_D}$ with Thermal noise

7.4.2 Shot noise

Shot noise in general, affects the pulse at the '1' level, so signal is bound to have noise at it's maximum level. In this investigation, we found effect of shot noise follow the similar pattern with respect to the plot with a lateral shift in the EOP of a signal without noise for each value of normalized length as shown in the Figure (7.13).

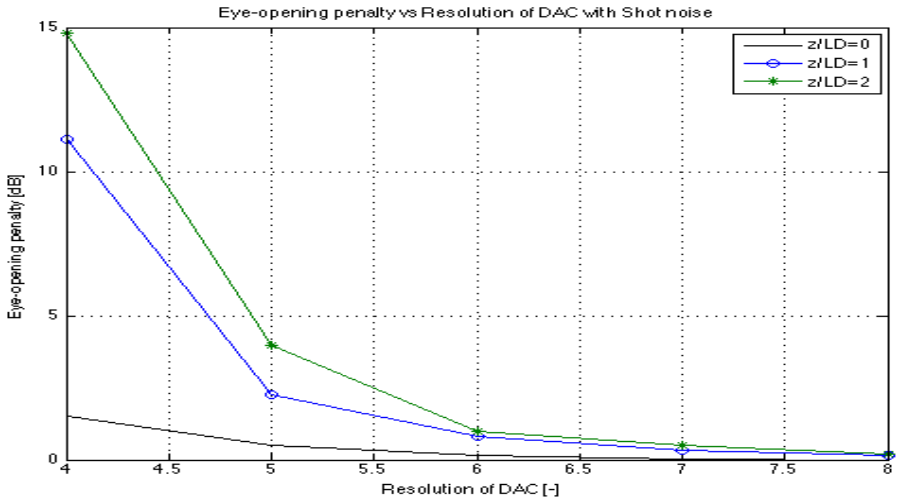

Figure 7.13: Eye-penalty vs Resolution of DAC for different values of normalized length $\frac{z}{L_D}$ with Shot noise

7.4.3 RIN

RIN measures the instability of power level of a continuous wave laser that drives a dual-drive MZM. RIN have slight effect on the EOP as compared to other noise parameters discussed above and is shown in the Figure (7.14).

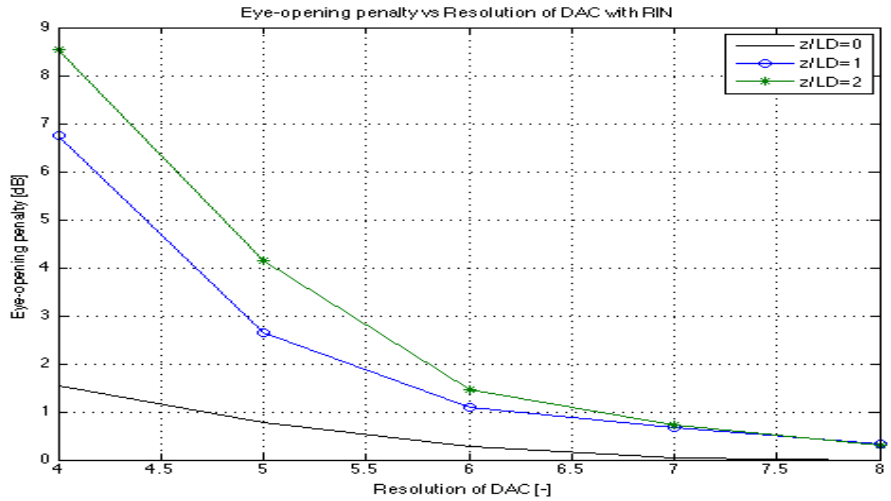

Figure 7.14: Eye-penalty vs Resolution of DAC for different values of normalized length $\frac{z}{L_D}$ with Shot noise

7.4.4 Total Noise

When all noise parameters are included, shape of the eye-opening plot remains the same, however, there is lateral shift indicating an increase in EOP as shown in the Figure (7.15).

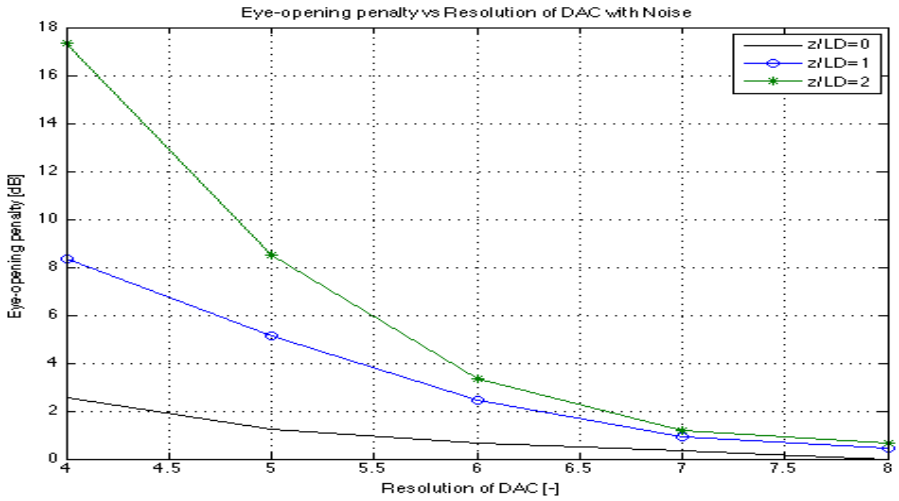

Figure 7.15: Eye-penalty vs Resolution of DAC for different values of normalized length $\frac{z}{L_D}$ with Shot noise

We know that in the presence of noise, signal degrades, however, it is also limited by the resolution of DAC. From the observations in the Figure (7.16), we can conclude that with respect to the resolution of the DAC, there is a tremendous increase in the EOP at resolution less than 5.

Chapter 8

Conclusion

We have successfully studied the analysis of pre-distortion technique both numerically and analytically using a gaussian pulse and a NRZ pulse encoding a $2^n - 1$ PRBS sequence. We can conclude that pre-distortion technique reverses the amount of linear dispersion in an optical fiber for any value of normalized length $\frac{z}{L_D}$ along the length of an optical fiber. Also to note that, this technique only works for compensating dispersion linearly ignoring the effects of attenuation and non-linear losses in an optical fiber. This gives an good conclusion that for distances more than dispersion length, if we include attenuation, power of signal could be diminished, but to overcome attenuation, it is safe to assume to use optical amplifiers at regular intervals along the length of an optical fiber.

From the analysis of a NRZ pulse, we studied the dependent nature of pre-distortion technique on the resolution of the DAC and order of the PRBS sequence, however, at the expense of heavy computational power. But due to increase in the availability of high speed processors and low power consumption electronics in the market, we can increase the order higher than 13 to yield better results to compensate the linear dispersion losses in the electrical domain. We have successfully investigated the effect of three types of noise in the pre-distortion technique and deducing the limitations of DAC from the plots as shown in Figure. From investigation, we can conclude that, to achieve any eye-opening penalty of signal less

than 2 [dB], resolution of DAC has to be greater than 5 which sets an limitation on the use of electrical component especially DAC in a pre-distortion technique.

Bibliography

[1] Robert I. Killey, Philip M. Watts, Vitaly Mikhailov, Madeleine Glick, and Polina Bayvel, *Electronic Dispersion Compensation by Signal Predistortion Using Digital processing and a Dual-Drive Mach-Zehnder Modulator.* IEEE Photonics Technology Letters, Vol. 17, no. 3, March 2005.

[2] Govind P. Agarwal, *Fiber-Optical Communications systems, Third Edition.*

[3] Govind P. Agarwal, *Nonlinear Fiber Optics, Fourth Edition.*

[4] Tingye Li, Alan E. Willner, Ivan Kamino, *Optical Fiber Telecommunications VA: Components and Subsystems.*

[5] Maria Morant,, Roberto Llorente, Jerome Hauden, Terence Quinlan, Alexandre Mottet, and Stuart Walker, *Dual-drive LiNbO3 interferometric Mach-Zehnder architecture with extended linear regime for high peak-to-average OFDM-based communication systems.*

[6] R. Udayakumar, V. Khanaa and T. Saravanan. *Chromatic Dispersion Compensation in Optical Fiber Communication System and its Simulation*

[7] Wei Chen *Chromatic Dispersion in Optical Fiber.* Rochester Institute of Technology, Rochester, New York, USA, October 15, 2011.

[8] D. McGhan, M. O?Sullivan, M. Sotoodeh, A. Savchenko, C. Bontu, M. Belanger, and K. Roberts. *Electronic dispersion compensation.* Optical Fiber Communication Conference, paper OWK1, 2006.

[9] J. H. Winters and R. D. Gitlin. *Electrical signal processing techniques in long-haul fiber-optic systems.* IEEE Transactions on Communications, vol. 38, no. 9, 1990.

[10] N. Henmi, T. Saito, and T. Ishida, *Prechirp technique as a linear dispersion compensation for ultrahigh-speed long-span intensity modulation direct detection optical communication systems* J. Lightw. Technol., Vol. 12, no. 10, Oct. 1994.

[11] H. Bulow, F. Buchali, and A. Klekamp, *Electronic dispersion compensation.* IEEE Journal of Lightwave Technology, vol. 26, no. 1, 2008.